

UNIVERZA V LJUBLJANI
FAKULTETA ZA FARMACIJO

NINA GERMIČ

MAGISTRSKA NALOGA

ENOVITI MAGISTRSKI ŠTUDIJ FARMACIJE

Ljubljana, 2014

UNIVERZA V LJUBLJANI
FAKULTETA ZA FARMACIJO

NINA GERMIČ

**LOKACIJA Z AVTOFAGIJO POVEZANEGA PROTEINA 12 V
CELICI**

**SUBCELLULAR LOCALIZATION OF AUTOPHAGY-RELATED
PROTEIN 12**

Ljubljana, 2014

The present master thesis was realized at the Institute of Pharmacology at the University of Bern, with collaboration of the Faculty of Pharmacy, University of Ljubljana. I worked under the supervision of Prof. Dr. Irena Mlinarič-Raščan and Prof. Dr. Dr. Hans-Uwe Simon.

Acknowledgment

I would like to express my gratefulness to Prof. Dr. Dr. Hans-Uwe Simon for giving me the opportunity to work in his research group. I thank him for the guidance through the project and continuous support, for his energy, motivation, immense knowledge and precious time to consider my work, which all appeared very inspiring.

I am very thankful to Dr. He Liu and Dr. Zhaoyue He who introduced me to research work for their assistance and support during everyday work, sharing their knowledge and enthusiasm with me. They helped me by motivating me to do my best and I consider myself very fortunate to work with them. I would like to thank Dr. He Liu for all the help and effort she put in reading and correcting my thesis as well as supporting me after my return from Bern.

I also wish to thank Prof. Dr. Irena Mlinarič-Raščan for her support, patience and guidance to complete the thesis. I deeply appreciate her energy and help for reading, correcting and improving my writings.

My thanks also go to all of the members at the Institute of Pharmacology at the University of Bern for creating a motivating and positive working environment.

Lastly, I would like to thank my family for being by my side throughout entire studies, encouraging me and believing in my work. They have always loved me and supported with patience which helped me to accomplish this project.

Statement

Hereby, I testify having performed the experiments to the best of my knowledge and having written this thesis independently under guidance of my supervisors: Prof. Dr. Irena Mlinarič-Raščan and Prof. Dr. Dr. Hans-Uwe Simon.

Ljubljana, May 2014

Nina Germič

President of the Thesis defence committee: Prof. Dr. Janko Kos

Member of the Thesis defence committee: Assist. Prof. Dr. Tihomir Tomašić

TABLE OF CONTENTS

TABLE OF FIGURES	V
ABSTRACT	VI
RAZŠIRJENI POVZETEK	VII
LIST OF USED ABBREVIATIONS	X
1. INTRODUCTION	1
1.1 AUTOPHAGY	1
1.1.1 <i>Introduction to autophagy</i>	1
1.1.2 <i>Types of autophagy</i>	1
1.1.3 <i>Molecular mechanism of autophagy</i>	2
1.1.4 <i>Autophagy in cancer</i>	5
1.1.5 <i>Methods to detect autophagy</i>	8
1.1.6 <i>Autophagy-related protein 12 (ATG12)</i>	9
1.2 MITOCHONDRIA	11
1.2.1 <i>Introduction to mitochondria</i>	11
1.2.2 <i>Mitochondrial biogenesis</i>	11
1.2.3 <i>Mitochondria and autophagy</i>	12
2. OBJECTIVES	13
3. MATERIALS AND METHODS	14
3.1 MATERIALS	14
3.2 METHODS.....	19
3.2.1 <i>Cell culture</i>	19
3.2.1.2 <i>Cell freezing</i>	20
3.2.1.3 <i>Cell thawing</i>	20
3.2.2 <i>Infecting cells with virus</i>	21
3.2.3 <i>Preparing cell lysate</i>	21
3.2.4 <i>Measuring the protein concentration</i>	22
3.2.5 <i>Western Blotting</i>	22
3.2.6 <i>Immunofluorescence staining</i>	24
3.2.7 <i>Subcellular fractionation</i>	25
3.2.8 <i>Quantification of the results</i>	26
3.2.8.1 <i>Quantification of protein expression on Western Blot</i>	26
3.2.8.2 <i>Colocalization analysis</i>	27
3.2.8.3 <i>Measuring mitochondrial area per cell</i>	27

4. RESULTS.....	28
4.1 ATG12 EXPRESSION WAS REDUCED UPON INDUCTION OF AUTOPHAGY BY STARVATION.	28
4.2 ATG12 WAS LOCALIZED ON MITOCHONDRIA.	32
4.3 DOWNREGULATION OF ATG12 LED TO REDUCED NUMBER OF MITOCHONDRIA.	40
5. DISCUSSION	45
6. CONCLUSION.....	49
7. REFERENCES.....	50

TABLE OF FIGURES

Figure 1: Schematic presentation of the autophagic process.....	4
Figure 2: Role of autophagy in tumor development.....	6
Figure 3: Role of autophagy in tumor promotion.....	7
Figure 4: Mechanism of ATG12-ATG5 conjugation in yeast.....	10
Figure 5: Levels of autophagy-related proteins after induction of autophagy.	30
Figure 6: ATG12 was not colocalized with LC3.	31
Figure 7: ATG12 was colocalized with Mitotracker.....	34
Figure 8: ATG12 was colocalized with MTC.	35
Figure 9: LC3 was not colocalized with Mitotracker.....	36
Figure 10: Significant difference between ATG12 staining with Mitotracker and LC3 staining with Mitotracker.	37
Figure 11: ATG12 was not colocalized with ATG5.	38
Figure 12: ATG12 was located in mitochondrial fraction.....	39
Figure 13: Downregulation of ATG12 by Lentivirus transfection.....	41
Figure 14: Morphological changes of cells with downregulation of ATG12.	42
Figure 15: Reduced mitochondrial number in cells with deficient ATG12 expression.	42
Figure 16: Significantly smaller area of mitochondria in cells with downregulation of ATG12.....	43
Figure 17: Reduced mitochondrial number in cells with downregulation of ATG12.....	44

ABSTRACT

Autophagy is a very well conserved catabolic process, continuously performed in the cells from yeast to mammals. It maintains the balance between synthesis and degradation of cellular constituents, assuring the homeostasis and providing optimal living conditions for organisms.

The autophagic machinery is regulated by autophagy-related (ATG) proteins, among which we focused on ATG12 since it has previously been shown in our lab that it is upregulated in several types of solid tumors. ATG12 is one of the key members in autophagy due to its role in ATG12-ATG5 conjugate which contributes to the elongation process of pre-autophagosomal membrane.

Numerous studies of autophagic role in cancer are ongoing with the purpose to provide a better insight into a complex autophagic mechanism and its functioning. In our project we intend to characterize ATG12 in human cancer cells with the main purpose to investigate the subcellular localization of ATG12. Experiments, conducted mainly by immunoblotting and fluorescence microscopy revealed the mitochondrial localization of ATG12.

We also demonstrate the potential role of ATG12 in mitochondrial biogenesis, which may contribute to tumor progression. Cells were infected with Lentivirus, containing the construct of shRNA for ATG12 to knockdown the expression of selected protein. Infected cells showed morphological changes in comparison to vector cells, they were larger and flatter, slowly detaching from the flask surface. The amount of mitochondria in cells with downregulation of ATG12 was significantly decreased, indicating the involvement of ATG12 in mitochondrial formation.

Since tumors acquire higher metabolic demands, increased number of mitochondria supports their growth with sufficient energy supply, which may explain the increased levels of ATG12 in tumor tissues found in our lab. Further studies are required to define how ATG12 affects mitochondrial biogenesis.

Taken together, our project contributes a tiny piece in mosaic of autophagy research, helping to understand the complex role of autophagic mechanism and its role in cancer.

Key words: *autophagy* ♦ *autophagy-related protein 12 (ATG12)* ♦ *cancer* ♦ *mitochondria*

RAZŠIRJENI POVZETEK

Avtofagija je evolucijsko zelo dobro ohranjen kataboličen proces, prisoten v celicah tako gliv kvasovk kot tudi sesalcev. Avtofagija ima pomembno vlogo pri vzdrževanju ravnotežja med sintezo in razgradnjo celičnih sestavin ter zagotavljanju celične homeostaze. V organizmu poteka ves čas na bazalnem nivoju, v primeru različnih stresnih dejavnikov, kot so hipoksija, pomanjkanje hranilnih snovi oz. rastnih faktorjev, prekomerna prisotnost reaktivnih kisikovih zvrsti ali okužba s patogeni, pa se intenzivnost procesa pospeši.

Začetek avtofagnega procesa vključuje nastanek dvojne membrane, ki zajame tarčni del citoplazme, namenjene za razgradnjo. Ta lahko vključuje odvečne in poškodovane celične organele, beljakovinske skupke ali patogene organizme. Po sklenitvi dvojne membrane nastane avtofagosom, za avtofagijo specifičen organel, ki se po združitvi z lizosomom preoblikuje v avto(fago)lizosom. Njegova vsebina se razgradi skupaj z notranjo membrano avtofagosoma. Razgradnja poteka s pomočjo hidrolizirajočih encimov, nastale organske molekule pa se vrnejo v citoplazmo, kjer služijo kot osnovni gradniki za izgradnjo novih celičnih sestavin. Proces razgradnje v avtolizosomih lahko ustavimo z dodatkom klorokina (CQ), ki zaradi dviga pH v lizosomih inhibira delovanje encimov.

Mehanizem avtofagije nadzorujejo z avtofagijo povezani (ATG) proteini, med katerimi sem se v magistrski nalogi osredotočila na protein ATG12. Zanj je bilo v naši raziskovalni skupini predhodno dokazano povečano izražanje v različnih vrstah tumorjev. ATG12 je sicer kot del konjugata ATG12-ATG5 udeležen pri podaljševanju pred-avtofagosomske membrane in je nepogrešljiv protein v procesu avtofagije.

Vloga avtofagije pri razvoju rakavih obolenj je aktualna tema številnih raziskav, katerih namen je omogočiti temeljit vpogled v delovanje in kompleksen mehanizem avtofagije. Njena zmanjšana aktivnost vodi v kopičenje poškodovanih organelov in ROS, ki lahko preko različnih mehanizmov povzročijo nastanek rakavih obolenj. Nasprotno pa avtofagija s pomočjo angiogeneze podpira rast že nastalih tumorjev in jih oskrbuje s kisikom ter hranilnimi snovmi.

Namen in eksperimentalni postopki

Namen predstavljene študije je čim boljše opredeliti protein ATG12 v človeških rakavih celicah. Prisotnost in nivo izražanja ATG12 po indukciji avtofagije smo ugotavljali z uporabo postopka za imunsko detekcijo proteinov po prenosu western ter s fluorescenčno mikroskopijo. Osredotočili smo se na določitev lokacije ATG12 v celicah, kar smo raziskovali s pomočjo fluorescenčne mikroskopije in celične frakcionacije. Po utišanju gena ATG12 smo preučevali vlogo ATG12 pri nastanku in rasti mitohondrijev s fluorescenčno mikroskopijo.

Študij avtofagije

V rakavih celicah kolona HCT116, pljuč H1299 in prsi MDA-MA-231 smo s stradanjem spodbudili avtofagijo ter ugotavljali morebitne spremembe v izražanju ATG12. Uspešnost spodbujene avtofagije smo ugotavljali s spremljanjem količine proteinov p62 in LC3. p62 se kot selektivni substrat za avtofagijo po indukciji omenjenega procesa pospešeno razgrajuje, kar zmanjša njegovo količino v celici. LC3 je specifičen označevalec avtofagosomov, saj se v obliki konjugata s fosfatidiletanolaminom (PE) nahaja na njihovi zunanji in notranji membrani. Povišana raven lipidiranega LC3 je pokazatelj povečane količine avtofagosomov in spodbujenega procesa avtofagije. V študiji smo dokazali uspešno indukcijo avtofagije ter hkratno zmanjšanje ravni ATG12 s prenosom western ter fluorescenčno mikroskopijo. S fluorescenčno mikroskopijo smo analizirali celične preparate in izračunali Pearsonov koeficient korelacije (R) med opazovanimi proteini. Majhen Pearsonov koeficient korelacije med ATG12 in LC3 je izražal nizko stopnjo kolokalizacije označenih proteinov. Opazili smo zanimiv vzorec nahajanja ATG12 v celici, saj se protein v nasprotju s pričakovanji večinoma ni nahajal na pred-avtofagosomskih strukturah skupaj z LC3.

V nadaljevanju nas je zanimala lokacija ATG12 v celici. Različne organele, kot so mitohondriji, lizosomi, endoplazmatski retikulum in aktinski filamenti, smo označili z zanje specifičnimi označevalci ter opazovali njihovo morebitno kolokalizacijo z ATG12. Rezultati naših raziskav so po opazovanju celičnih preparatov s fluorescenčno mikroskopijo pokazali, da se ATG12 nahaja na mitohondrijih.

Mitohondrije in LC3 smo imunofluorescenčno označili ter s fluorescenčno mikroskopijo ugotavljali medsebojno kolokalizacijo. Rezultati so skladno z našimi pričakovanji pokazali nizko stopnjo ujemanja, saj se LC3 ne nahaja na mitohondrijih, temveč na avtofagosomih.

Nadaljevali smo z imunofluorescenčnim označevanjem proteinov ATG12 in ATG5. Kot je znano, se ATG12-ATG5 konjugat nahaja na pred-avtofagosomskih membranah, zaradi česar smo pričakovali visoko stopnjo kolokalizacije proteinov. Analiza rezultatov je razkrila zelo nizko raven ujemanja lokacije ATG12 in ATG5, kar kaže na ločeno mesto njunega nahajanja v celici.

Lokacijo ATG12 smo preverjali s celično frakcionacijo, s katero smo ločili mitohondrije od preostalih celičnih komponent. Za uspešno določitev lokacije ATG12 smo najprej dokazali zadostno ločitev in čistoto posameznih frakcij. Medtem ko smo protitelo LAMP-1 za lizosomski protein detektirali le v lizosomski frakciji, smo protitelo MTC za mitohondrijski protein opazili le v mitohondrijski frakciji. Nelipidiran LC3 smo pričakovano detektirali le v citosolni in lizosomski frakciji ter na podlagi rezultatov sklepali na uspešno frakcionacijo. Prisotnost ATG12 smo opazili le v mitohondrijski frakciji, kar je potrdilo naše dotedanje rezultate o prisotnosti preiskovanega proteina na mitohondrijih.

V nadaljnjih poskusih smo ugotavljali potencialno vlogo ATG12 pri nastanku in razvoju mitohondrijev, s čimer bi lahko ATG12 prispeval k napredovanju in širjenju rakavih obolenj. Z Lentivirusom smo v celice vnesli shRNA konstrukt za zavrtje izražanje ATG12. Opazili smo nastanek morfoloških sprememb v celicah, ki so postajale večje, bolj ploščate ter se počasi ločevale od površine, na katero so bile pritrjene. Število mitohondrijev se je v celicah z zavrtim izražanjem ATG12 znatno zmanjšalo, kar nakazuje na vpletenost ATG12 pri nastanku in rasti mitohondrijev.

Za tumorje je značilna povišana intenzivnost metabolnih procesov ter s tem tudi povečana potreba po energiji, kisiku in hranilnih snoveh. Mitohondriji jim z zagotavljanjem zadostne količine energije pomagajo preživeti, s čimer bi lahko razložili povišan nivo izražanja ATG12 v rakavih tkivih. Za natančnejšo opredelitev vloge ATG12 pri biogenezi mitohondrijev so potrebne nadaljnje študije.

Če povzamemo, naš projekt prispeva majhen košček k razumevanju kompleksnega mehanizma avtofagije ter njene vloge pri rakavih obolenjih.

Ključne besede: *avtofagija ♦ z avtofagijo povezan protein 12 (ATG12) ♦ rak ♦ mitohondriji*

LIST OF USED ABBREVIATIONS

ATG	Autophagy-related
BCA	Bicinchoninic acid
BSA	Bovine serum albumin
CQ	Chloroquine
DAPI	4',6-Diamidino-2-Phenylindole
DMSO	Dimethyl sulfoxide
DTT	Dithiothreitol
EBSS	Earle's Balanced Salt Solution
EDTA	Diaminoethane-tetraacetic acid
FCS	Fetal calf serum
GFP	Green fluorescent protein
mtDNA	Mitochondrial DNA
mTOR	Mammalian target of rapamycin
PBS	Phosphate-buffered saline
PE	Phosphatidylethanolamine
PFA	Paraformaldehyde
PI3K	Phosphoinositide 3-kinase
PGC-1 α	Peroxisome proliferator-activated receptor gamma coactivator 1-alpha
PMSF	Phenylmethanesulfonylfluoride
R	Pearson's correlation coefficient
ROS	Reactive oxygen species
RT	Room temperature
SDS-PAGE	Sodium dodecyl sulfate polyacrylamide gel electrophoresis
TBS	Tris-buffered saline

1. INTRODUCTION

1.1 Autophagy

1.1.1 Introduction to autophagy

Autophagy is a regulated catabolic process by which the redundant cell constituents are digested by lysosomal degradation in order to assure enough energy and basic molecular elements for cell survival. Cells deliver their damaged organelles, protein aggregates and pathogens to lysosomes, where they are eliminated by autophagic pathway (1, 2).

Autophagy is well conserved through the evolution, occurring in all eukaryotic organisms, from yeast to mammals. Under normal conditions, autophagy is constantly maintained at a basal level. As a dynamic process of continuous synthesis and degradation it assures cell homeostasis. It is induced in stress conditions such as starvation, growth factors withdrawal, hypoxia, by reactive oxygen species, infections with pathogens and anti-cancer therapy. Thereby autophagic pathway may serve as a survival mechanism in critical conditions. It also has a great role in various biological mechanisms including cell survival, cell metabolism, development, ageing and immunity (1-5).

1.1.2 Types of autophagy

Three different types of self-digestion have been described, including macroautophagy, microautophagy and chaperone-mediated autophagy. The major pathway is macroautophagy, where part of the targeted cytoplasm is sequestered by the unique membrane structure, termed autophagosome. It is a double-membrane vesicle, which merges with the lysosome (1, 2, 3). Lysosomes are small, irregularly shaped organelles, containing hydrolytic enzymes for intracellular digestion of proteins, nucleic acids, oligosaccharides and lipids (6). Fused together with the autophagic vacuole they generate an auto(phago)lysosome. The cell contents, as well as the inner autophagosomal membrane, are degraded and released back into the cytoplasm. In microautophagy, a smaller fraction of cytoplasmic material is sequestered directly by a lysosome, without preforming the autophagosomal structure. Chaperone-mediated autophagy is the most selective process, indicated only for soluble, long-lived proteins. These are directly transferred across the lysosomal membrane with the assistance of chaperones and lysosomal receptor proteins (1, 2, 3, 7).

In master thesis we will focus on macroautophagy and for the purpose of simplicity, we will relate to it as autophagy.

1.1.3 Molecular mechanism of autophagy

Autophagic process is controlled by autophagy-related (ATG) genes (1, 2, 6). Up to now, 37 different ATG genes have been recognized in yeast. Among these, 19 ATG genes participate in mammalian autophagy, hence they are named core genes (ATG 1-10, 12-18, 101, Vps34) (5).

Crucial role in regulating autophagy has a mammalian target of rapamycin (mTOR). When the levels of nutrients and energy in cells are sufficient, mTOR inhibits the kinase activity of ATG1 complex by its phosphorylation, leading to the inhibition of autophagy. On the contrary, if the nutrients are lacking, mTOR induces the autophagic process (1, 7, 8). Next, important regulators of autophagy are also class I and class III phosphoinositide 3-kinase (PI3K) pathways. Class I PI3K has the same effect as activated mTOR and inhibits the initiation of autophagy, while class III PI3K promotes the induction of autophagy (1).

Drug rapamycin, also known as sirolimus (Rapamune®) is a macrolide antibiotic used as an immunosuppressive agent and it is approved for the treatment of organ transplant patients. Its antiproliferative functions are due to interleukin-2 inhibition, which prevents growth and differentiation of T lymphocytes. Rapamycin inhibits the mTOR signaling pathways and induces autophagy, promoting the protective functions of autophagy, such as removal of damaged organelles. It is involved in many clinical trials since it may serve as a potential target in treatment of neurodegenerative, cardiac and cancer diseases (9, 10, 11).

The autophagic process consists of three principal phases, referred to as initiation, elongation and degradation (1). First is the so-called initiative step, where the formation of autophagosome is induced just after the mTOR inhibition of ATG1 complex is blocked. What follows is the nucleation as the autophagosomal membrane starts to form with the assistance of different proteins. Beclin 1 has a significant role in the regulation of autophagy. By binding in a complex with Vsp34 (class III PI3K) it increases the Vsp34 activity and consequently induces autophagy. Other proteins like UVRAG, AMBRA1 and Bif1 promote the formation of autophagosome, whereas protein Bcl-2 inhibits it. In short, activation of Vsp34 complex is essential for successful vesicle nucleation. Elongation step involves the expansion and closure of expanding membrane, resulting in completed

autophagosomal formation. Formation of a double-membrane organelle requires two protein conjugation systems, essential for elongation phase. One involves covalently linked ATG12-ATG5 conjugate, which dissociates from the outer autophagosomal membrane after vesicle formation is completed. The other conjugation system includes LC3, which is cleaved upon autophagy and results in cytoplasmic LC3-I. It gets lipidated into LC3-II after interaction with phospholipid phosphatidylethanolamine (PE). Recently formed conjugation complex is integrated into both, inner and outer autophagosomal membrane. Since LC3-II is present in formed autophagosome, it is a commonly used marker for detection of double-membrane autophagic organelle. Final step, when completed autophagosome fuses with the lysosome, is called degradation. Autolysosomal content is degraded by lysosomal hydrolytic enzymes (Figure 1) (1, 7, 8, 12).

Chemicals, such as chloroquine and ammonium ions are weak bases, raising the pH value in lysosomes, deactivating enzymes and consequently disabling degradation of vesicle cargo (Figure 1). As a drug was chloroquine (Aralen®, Arechin®, Resochin®) primarily used for the treatment of malaria (13, 14). Due to its mildly expressed immunosuppressive functions it may be used in some autoimmune diseases, such as rheumatoid arthritis. Chloroquine is being investigated as a potential drug for cancer treatment since the inhibition of autolysosome degradation prevents elimination of metabolic stress products and induces programmed cell death in tumors (13, 14, 15).

Bafilomycin regulates intracellular pH by acting as a strong and specific inhibitor of a vacuolar H⁺ ATPase, known as a proton pump (Figure 1) (16). Protein p62 has a variety of cellular functions, mainly in signaling and degradation pathways. Current studies suggest it might be important in neurodegenerative diseases and tumorigenesis as well (16, 17, 18). Since protein p62 is generally degraded by autophagy and accumulates while autophagy is inhibited, the reduction of p62 indicates successful vesicle degradation (18, 19).

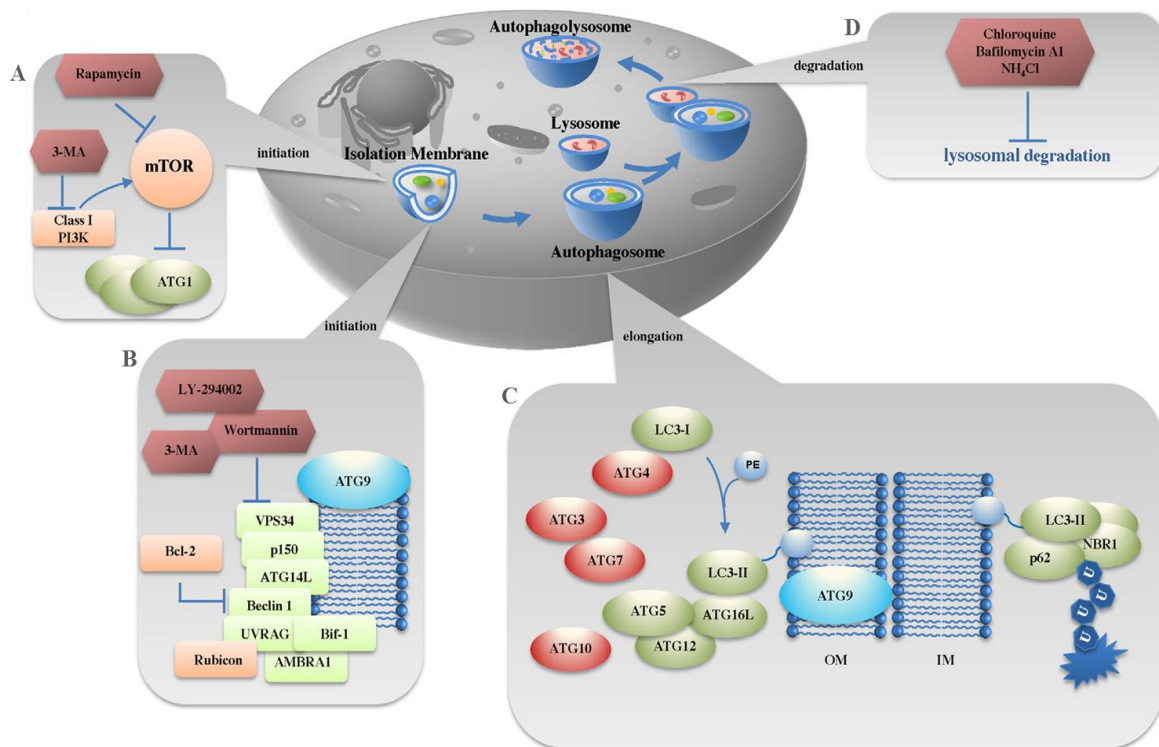


Figure 1: Schematic presentation of the autophagic process. The whole machinery is regulated by four functional subgroups of ATG proteins. **A** First set of proteins, ATG1 (ULK1 in mammals), ATG13 and ATG17, is responsible for the initiation of autophagy. It may be inhibited by the action of class I PI3K or mTOR. Drug rapamycin works as mTOR inhibitor and therefore induces autophagy. **B** Next, nucleation of autophagosomal membrane is regulated by ATG proteins Beclin1 (ATG6 in yeast), ATG14 and ATG9. Beclin1 and ATG14 are joined in a complex with several different proteins, including class III PI3K (Vsp34), p150, UVRAG, Bif-1, AMBRA1 and Rubicon. **C** ATG proteins from the third group are involved in two conjugation systems, characterizing the elongation process. ATG12 covalently binds to ATG5 with the assistance of ATG7 and ATG10 enzymes and forms a complex through interaction with ATG16L (ATG16 in yeast). Second conjugation system encompasses the sequence of events, leading to conjugation of LC3 (ATG8 in yeast) with PE. Lipidated LC3-II exists as a part of the autophagosomal membrane. The fourth group of ATG proteins consists of ATG2, ATG9 and ATG18. Their responsibility is to recruit other ATG proteins to participate in autophagic machinery. **D** Chemical agents such as chloroquine and bafilomycin can inhibit degradation of autolysosomes (1).

1.1.4 Autophagy in cancer

Interestingly, researches have shown that autophagy exhibits two different functions in cancer evolution. Primarily autophagy serves as a tumor suppressor mechanism, protecting cells and maintaining homeostasis under both, normal and stress conditions. On the contrary, autophagic pathway supports promotion of established tumors by providing them with a favorable living environment (20, 21, 22).

Autophagy as a survival process degrades and recycles both broken or excessive macromolecules and organelles. It ensures sufficient levels of building blocks and energy for cell survival. Inadequate autophagy causes various aberrations, such as accumulation of harmful material, including dysfunctional mitochondria, protein p62 and unfolded proteins. Accordingly to listed facts, defects lead to the development of oxidative stress, reactive oxygen species (ROS) production and genome instability. Genome integrity is weaker as damages of DNA occur more frequently. Cells which undergo unpleasant metabolic conditions experience a higher number of mutations and therefore promote tumor formation through induced oncogene activation (20, 21). Further, sufficient autophagy may restrain tumorigenesis by promoting oncogene-induced senescence (OIS). As a result, proliferation of damaged cells is limited, while deficient autophagy and therefore decreased clearance of mutations lead to malignant alterations (20, 21, 24). Another mechanism that might cause cancer and is related to autophagy is temporary arrest of both, apoptosis and autophagy. Cells are obligated to undergo cell death by necrosis, causing infiltration of inflammatory factors, hence contributing to tumor development (Figure 2) (7, 20). Several alterations of ATG protein expression have frequently been discovered in assorted human tumors. As supporting evidence may serve mono-allelic loss of tumor suppressor genes, such as Beclin-1 (found in breast, ovarian and prostate cancer) or UVRAG (found in colon cancer) (3). In addition, reduction of ATG5 expression, indicating defective autophagic pathway, was observed in many patients with malignant melanomas (24).

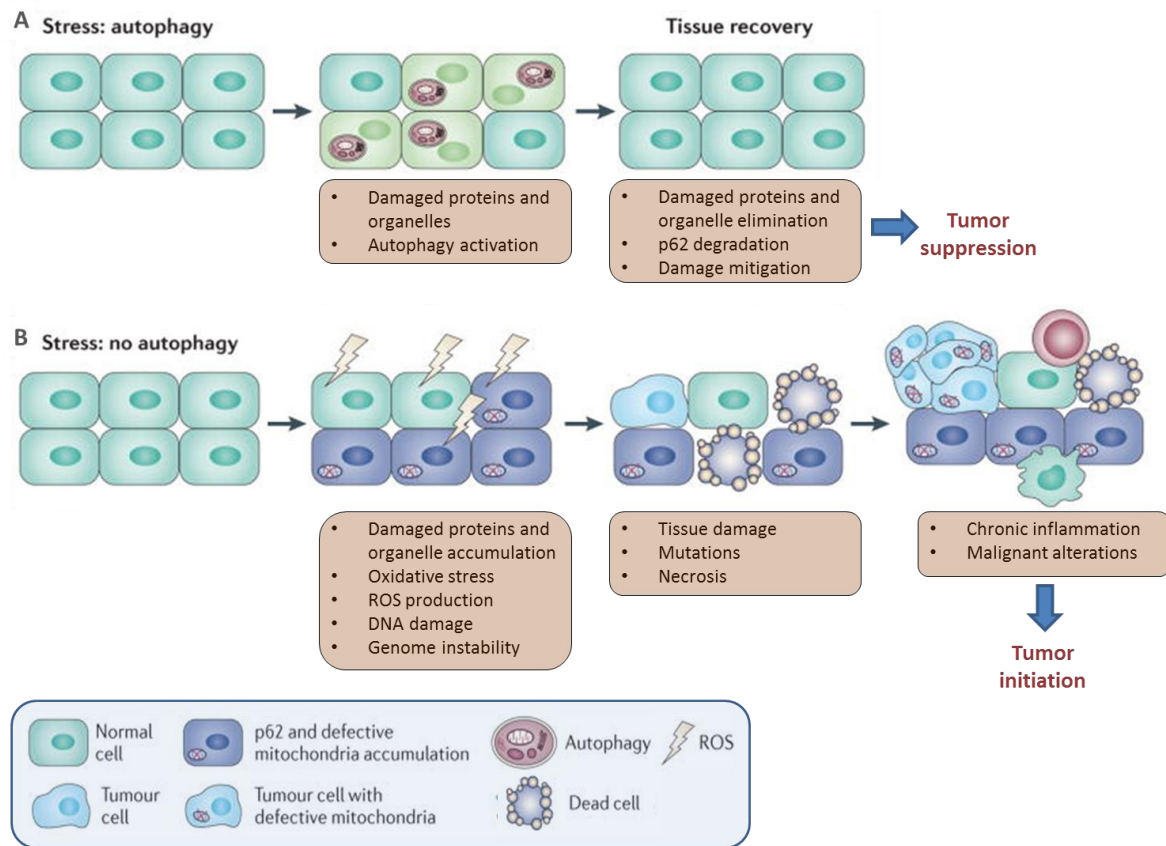


Figure 2: Role of autophagy in tumor development. **A** Sufficient autophagy leads to tumor suppression due to elimination of damaged cell constituents and prevention of oncogenic proteins accumulation. **B** Insufficient autophagy levels cause cellular stress which leads to chronic tissue damage and tumor initiation (adapted from 30).

Autophagy can exhibit also the opposite effect from the one discussed above and thus enable survival of tumor cells, particularly in advanced cancers. Growth of tumor is commonly rapid and aggressive with high demands for nutrients and oxygen. Inner parts in the center of the tumor mass are eventually undergoing metabolic stress, caused by starvation and hypoxia for the reason of insufficient blood supply. Defective cells can recover through upregulation of autophagy since it stimulates angiogenesis and tumor promotion is able to continue (Figure 3) (7, 25, 26). Studies of human pancreatic cancers revealed elevated levels of autophagy in malignant cells and generation of tumorigenesis, while inhibition of autophagic machinery restrained growth of pancreatic tumor (27). Next, increased regulation of autophagy was observed in cancers with oncogenic mutation of Ras gene. These alterations are frequently present in a variety of cancers, affecting lung, colon,

pancreatic, skin, bladder or bone marrow tissues (28). Ras activated cancers, along with many others, express increased levels of basal autophagy as they need to meet demands of extensive cell metabolism and growth. They are autophagy-dependent and hence highly responsive to inhibition of this process (27, 29, 30). Large amounts of cellular stress might be produced by anticancer therapy as well. Cells raise level of autophagy to ensure clearance of unwanted, toxic agents and therefore reduce the effectiveness of treatment. As demonstrated in melanoma cells, tumors with more intense autophagy showed weak response to therapy, which turned to be less effective as expected (31). Furthermore, autophagy helps cancer cells to overcome programmed cell death, termed anoikis. As follows, cells survive separately from the extracellular matrix and since they are detached, they spread and form metastasis through the organism (24, 32).

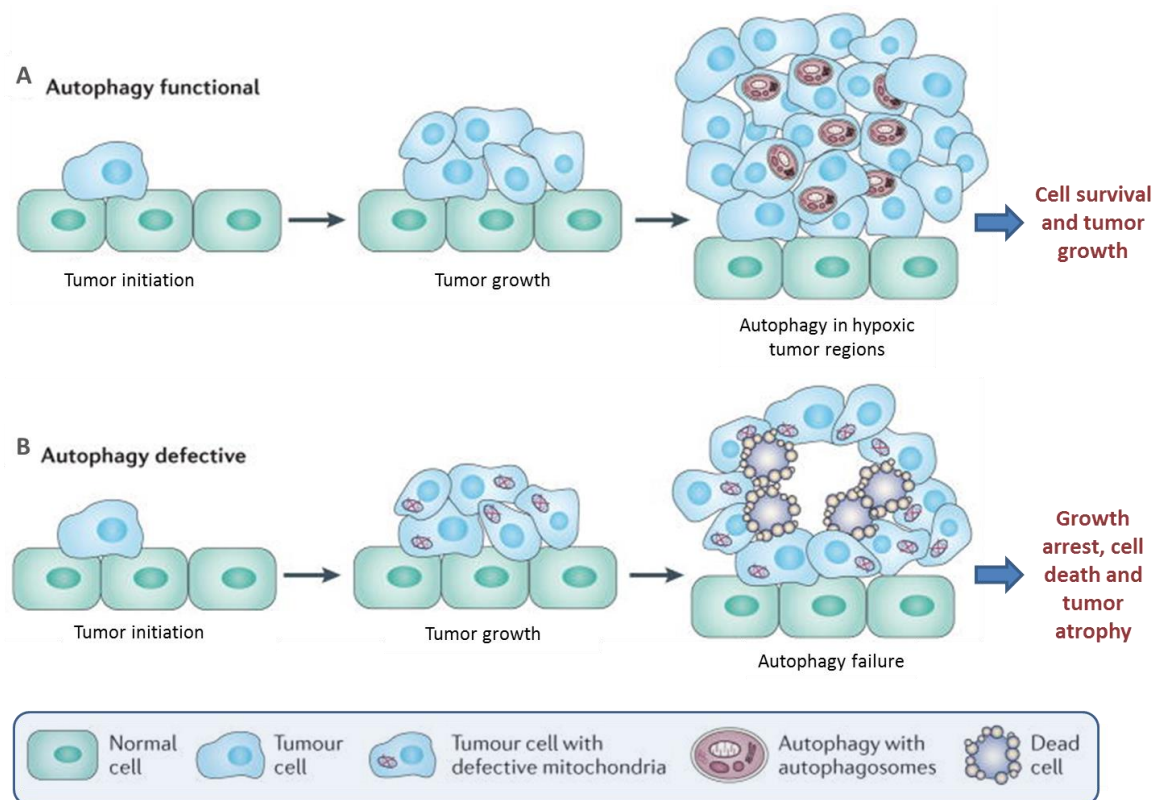


Figure 3: Role of autophagy in tumor promotion. **A** Once the tumor is formed, autophagy contributes to survival of hypoxic regions, promotes angiogenesis and supports tumor growth. **B** Defective autophagy may promote cell death of tumor cells due to accumulation of damaged proteins and excessive oxidative stress (adapted from 30).

Taken together, a deeper view of autophagic role in tumorigenesis reveals its high complexity. Modulation of autophagy has a great potential in cancer treatment, varying with different type and stage of individual tumor.

1.1.5 Methods to detect autophagy

Over the last decade, interest in autophagy has remarkably increased. As the amount of studies is growing, proper understanding of measurement techniques for reliable results is required. Main methods to monitor autophagy are based on electron microscopy, fluorescence microscopy and biochemical techniques, such as immunoblotting (33).

First observations of autophagic process in 1950s were detected with electron microscope, which is today considered as a standard approach. It is based on morphological identification of autophagic vesicles (34). Autophagosome is recognized as a double-membrane organelle, which consists of engulfed, easily identified cytoplasmic structures (33, 35). In case of selective autophagy, specific cargo such as mitochondria (mitophagy), peroxisomes (pexophagy), endoplasmic reticulum (reticulophagy), ribosomes (ribophagy) or pathogens (xenophagy) is captured in vesicles and hence only certain substrates are visualized (36). It is more delicate to recognize autolysosomes since they are limited with a single membrane and contain materials at different stages of degradation. Quantification may be accomplished by counting autophagic structures or rather assessing their volume with suitable assays (33).

LC3-II is a specific marker for autophagosomes, located on its outer and inner membrane (20, 35). Level of LC3 is observed with fluorescence microscopy, most commonly directly through green fluorescent protein (GFP) or indirectly by labelling with antibody (33, 37). GFP is linked to N-terminus of LC3 and observation of fluorescent dots indicates the presence of autophagosomes (33).

Quantification of LC3 puncta is displayed as the number of cells expressing dots or rather as the number of dots per cell, which may be more accurate and sensitive (33, 35). Improved estimation of the dynamic autophagic process is achieved by mRFP-GFP reporter, tagged to LC3. Since GFP fluorescence is sensitive to lower pH, it is quenched in autolysosomes where no signal is detected. On the contrary, fluorescence of monomeric red fluorescent protein (mRFP) is still stable in acidic pH, and positive dots are visible in both, autophagosomes and autolysosomes (33, 38, 39). Fluorescence microscopy may be

applied to immunohistochemistry as well. Antibodies are conjugated to a fluorophore and used to label selected endogenous protein in tissue sections, particularly LC3 to monitor autophagy (33).

Further, different amounts of LC3 can be observed by western blotting, using specific anti-LC3 antibodies. Conversion from cytosolic LC3-I to lipidated LC3-II indicates the autophagic activity. As LC3-II is located on autophagosomal membrane, levels of LC3-II correspond to the number of autophagosomes. Fusion with a lysosome is followed by the removal of LC3-II from the outer membrane, while LC3-II from the inner membrane proceeds through degradation pathway (33, 38, 40, 41). Separation of proteins in SDS-PAGE (sodium dodecyl sulfate polyacrylamide gel electrophoresis) is based on their size. In immunoblotting LC3 is identified with two bands. LC3-II has a greater molecular mass as it binds to phosphatidylethanolamine (PE), but migrates faster than LC3-I due to its high hydrophobicity (38, 41).

Regarding quantification, it is preferred to express LC3-II level by comparing it to LC3-I, which is described as LC3-II/LC3I ratio (33). Alternatively, other substrates such as p62 might be used to measure autophagic flux (33, 38).

While monitoring autophagy, it is important to critically evaluate the results. Autophagy is not considered as static, but rather a dynamic degradation process. Improved imitation of actual process is assured with the usage of various time points and/or inhibitors for vesicle degradation. Since there is no standard assay to accurately measure autophagic activity, combination of different methods is recommended (33).

1.1.6 Autophagy-related protein 12 (ATG12)

ATG12 is one of the main factors participating in elongation and formation of autophagosomal membrane. With the assistance of two enzymes, ATG7 and ATG10, it covalently binds to ATG5. Further, ATG16L interacts with ATG5 and triggers transport of ATG12-ATG5 from cytosol to the site of membrane formation (Figure 4). Complex is mainly positioned on the outer side of expanding membrane and at the time of autophagosome completion it dissociates from the membrane, moving back to cytosol (8, 42, 43, 44). ATG12-ATG5-ATG16L assembles with homologous units, forming a multimeric complex due to ATG16L self-oligomerization. It exhibits a ligase activity by both, enhanced transfer of LC3-I from ATG3 to phospholipid PE and interaction between

ATG12 and ATG3, retrieving ATG3 to the membrane site. Taken together, an ATG12-ATG5-ATG16L complex enables LC3-I lipidation and functions as a crucial component in both conjugation systems (42, 45, 47). Interestingly, an ATG12-ATG3 conjugate was reported to participate in mitochondrial homeostasis and quality control, without having an evident function in autophagy. It was shown that defective ATG12-ATG3 conjugate resulted in impaired mitochondrial apoptotic pathway (47, 48).

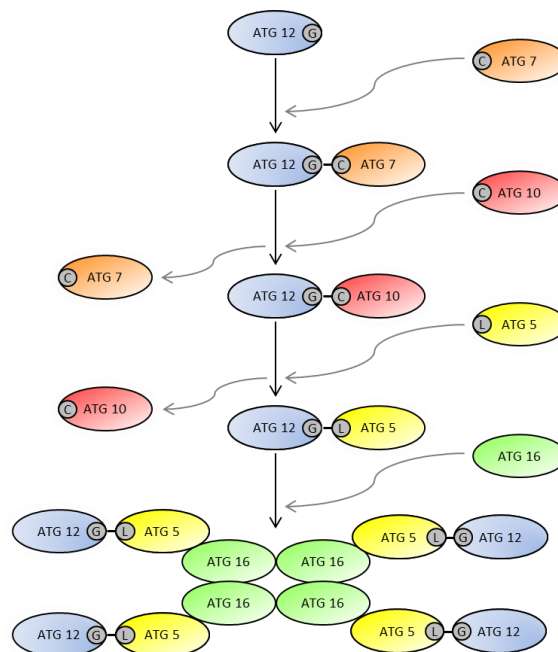


Figure 4: Mechanism of ATG12-ATG5 conjugation in yeast. First, ATG12 is activated by forming a thioester with ATG7. Activated ATG12 is carried to ATG10 and after cleavage of ATG7, ATG12 joins with ATG10, forming a thioester linkage. Since ATG10 serves as a conjugation enzyme, it promotes formation of ATG12-ATG5 conjugate through formation of an isopeptide bond. Upon non-covalent interaction with ATG5, ATG16 assembles with a conjugate and forms a tetramer of the ATG12-ATG5-ATG16 conjugates (8).

Western blotting of ATG12 reveals the existence of two bands at different molecular weights. The higher one at 55 kDa represents an ATG12-ATG5 conjugate, while the lower one at 21 kDa belongs to a single ATG12 (2, 47, 50). A great part of ATG12 is present in a complex with ATG5, which is mostly located in cytosol while the rest associates with nascent autophagosomal membrane. A research about subcellular localization of ATG12

and ATG5 by differential centrifugation revealed that single ATG5 and ATG12-ATG5 conjugate appeared in the same dense fraction while ATG12 emerged in denser fractions. Results suggest that upon induction of autophagy ATG12 needs to be translocated to the cellular compartment of ATG5 in order to form a conjugate ATG12-ATG5 (44, 49, 50).

1.2 Mitochondria

1.2.1 Introduction to mitochondria

Mitochondria are one of the most prominent organelles in eukaryotic cells. Their number, shape and location vary depending on cellular demands. Mitochondria are enclosed by a double membrane system. The outer membrane contains porins, protein channels, which regulate permeability of small molecules. Contrary, the inner membrane has highly limited permeability. It is extensively folded and includes protein complexes that are essential for energy production (6, 51). The largest source of energy for cell survival is assured by mitochondria, generating ATP through the linking of oxidative phosphorylation with electron transport. Next, mitochondria are the main producers of intracellular ROS and also their prime targets. Mitochondria may also contribute to cell death upon different mechanisms, such as interruption of electron transport, release of cytochrome c to the cytosol or altered expression of apoptotic proteins. Taken together, mitochondria have a significant role in regulation of cell survival (6, 51, 52, 53).

1.2.2 Mitochondrial biogenesis

One of mitochondrial structural characteristics is the existence of its own genome, encoded in mitochondrial DNA (mtDNA), a circular double-stranded molecule. It consists of 37 genes and 13 of them code for proteins, involved in a respiratory chain on the inner mitochondrial membrane. The rest of genes encode 22 transfer RNAs and 2 ribosomal RNAs, needed for the translation process of mitochondrial messenger RNA in matrix. However, majority of the proteins residing in mitochondria are products of nuclear genome, hence they are synthesized in cytosol and imported into mitochondria. Coordination of mitochondrial and nuclear gene expression is controlled by various regulatory factors and is required for proper mitochondrial biogenesis (6, 51-55).

1.2.3 Mitochondria and autophagy

Autophagy is an indispensable mechanism, required for preserving normal mitochondrial functions. It eliminates damaged or excessive mitochondria through mitophagy and maintains a balance between formation and degradation of organelles. In case of starvation, autophagy provides nutrients such as fatty acids and amino acids for normal acetyl-CoA synthesis, followed by tricarboxylic acid (TCA) cycle (30, 56). Insufficient substrate supply may lead to increased glycolysis (Warburg metabolism) or glutaminolysis (57). Further, impaired autophagy results in accumulation of defective mitochondria, excessive ROS production and dysfunction of both energy production and apoptosis regulation (58). Consequently, autophagy may contribute to tumor promotion and becomes necessary for their growth (30, 56).

2. OBJECTIVES

My research work is based on results, gained from previous experiments with tumor tissue microarrays. Tissue microarray is a collection of multiple tissue samples from different patients, assembled on one slide. It represents a high throughput technique that enables distribution and expression studies of a specific biomarker (59, 60). Our tissue microarray contained a pair of tumor and corresponding normal tissue from each of numerous patients. Samples were stained with different autophagy-related proteins by performing immunohistochemistry. Among them, ATG12 was seen to be upregulated in tumor tissues in comparison to their corresponding normal tissues. Also an interesting staining pattern of ATG12 was observed.

The aim of research presented in this thesis is to characterize autophagy-related protein 12 in tumors. I shall evaluate whether induction of autophagy affects cellular levels of ATG12 in human cancer cells. Next, I will determine subcellular localization of ATG12 and elaborate on its function. Our main methods to conduct experiments will be immunoblotting and immunofluorescence staining, followed by microscopy.

3. MATERIALS AND METHODS

3.1 Materials

Table I: Machines used in experiments

Machine	Type	Company
Incubator	Heraeus HERAcell 150i	Thermo Fisher Scientific
Centrifuge	Heraeus Multifuge 3SR	Thermo Fisher Scientific
Microcentrifuge	Centrifuge 5417 C	Eppendorf
Microcentrifuge	Centrifuge 5417 R	Eppendorf
Thermomixer	Thermomixer compact	Eppendorf
Vortex mixer	Vortex-Genie 2	Scientific Industries
Electrophoresis machine	Powerpac 3000	BioRad
Electronic analytical balance	XP205	Mettler Toledo
Microplate reader	SpectraMax M2	Molecular Devices
Western Imaging System	Odyssey Fc	LI-COR Biosciences
Imaging System	X-Omat 2000 processor	Kodak
Light microscope (inverted fluorescent)	Zeiss Axiovert 35	Carl Zeiss
Confocal microscope	LSM 5 Exciter	Carl Zeiss
Freezer (-20°C)	G 3513	Liebherr
Freezer (-80°C)	MDF-5386SC	Sanyo

Table II: Devices used in experiments

Devices	Type	Company
Pipettes	2.5 μ L, 10 μ L, 100 μ L, 1000 μ L	Eppendorf
Micro Test Tube	3810X; 1.5 mL	Eppendorf
Serological pipettes	5 mL, 10 mL, 25 mL	Eppendorf
Aspirating pipette	2 mL	Greiner Bio-One
Cryogenic vial	Nunc CryoTubes; 1.8 mL	Sigma
Pipette boy	Pipetboy acu	INTEGRA Biosciences
Falcon tubes	PP tubes with screw cup; 15 mL, 50 mL	Greiner Bio-One
Cell culture plates	6-, 24- and 96-well plates	Greiner Bio-One
Cell culture flasks	TC Flasks with filter cap (50 mL, 250 mL, 550 mL)	Greiner Bio-One
Cytoslides	Shandon Single Cytoslides	Thermo Scientific
Electrophoresis System	XCell SureLoc Mini-Cell	Life Technologies
Autoradiography film	Amersham Hyperfilm ECL	GE Healthcare
Transfer membrane	Immobilon – P	EMD Millipore
Transfer membrane	Immobilon – FL	EMD Millipore
Counting chamber	Neubauer Improved	Assistent

Table III: Media and chemicals used in experiments

Media and chemicals	Company
DMEM + GlutaMAX (Dulbecco's Modified Eagle Medium)	Invitrogen, Life Technologies
RPMI Medium 1640 + GlutaMAX	Invitrogen, Life Technologies
McCoy's 5A + GlutaMAX (Modified Medium)	Invitrogen, Life Technologies
FCS	PAA Laboratories
Penicillin-Streptomycin	Invitrogen, Life Technologies
PBS	PAA Laboratories
Trypsin	Life Technologies
Protease inhibitor cocktail (104 mM AEBSF, 80 μ M Aprotinin, 4 mM Bestatin, 1.4 mM E-64, 2 mM Leupeptin, 1.5 mM Pepstatin A)	Sigma
Pierce BCA Protein Assay Kit	Thermo Scientific
NuPAGE LDS Sample Buffer (4X)	Life Technologies
RunBlue SDS Running Buffer (20X)	Expedeon
Restore Western Blot Stripping Buffer	Thermo Scientific
RunBlue 12% SDS PAGE Precast Gel	Expedeon
Pre-Stained Protein Standard Novex Sharp	Life Technologies
Western Blotting Reagent Luminata Forte	EMD Millipore

Pierce ECL Plus Western Blotting Substrate	Thermo Scientific
Amersham ECL Prime Western Blotting Detection Reagent	GE Healthcare
BSA Fraction V Solution (7.5%)	Life Technologies
ProLong Gold Antifade Reagent with DAPI	Life Technologies
EBSS	Life Technologies
Chloroquine	Sigma
Mitotracker Orange (CMTMRos)	Life Technologies
Rabbit ATG1 Antibody (ULK-1)	Sigma
Rabbit ATG7 Antibody	Abgent
Mouse ATG12 Antibody	R&D Systems
Mouse ATG5 Antibody (7C6)	NanoTool
Mouse p62 Antibody	Santa Cruz Biotechnology
Mouse GAPDH Antibody	EMD Millipore
Mouse LC3 Antibody	NanoTool
Mouse MTC Antibody	Abcam
Rabbit LAMP-1 Antibody	Abcam
Rabbit ATG12 Antibody	Cell Signaling Technology
Rabbit LC3 Antibody	Cell Signaling Technology

Rabbit ATG5 Antibody	LSBio
Mouse ATG5 Antibody (11C3)	NanoTool
Secondary fluorescent mouse Antibody from goat	LI-COR Biosciences
Secondary fluorescent rabbit Antibody from goat	LI-COR Biosciences
ECL Mouse IgG, HRP-linked whole Antibody from sheep	GE Healthcare
ECL Rabbit IgG, HRP-linked whole Antibody from donkey	GE Healthcare
Goat-anti-mouse Antibody, 555	Invitrogen, Molecular Probes
Goat-anti-mouse Antibody, 488	Invitrogen, Molecular Probes
Goat-anti-rabbit Antibody, 568	Invitrogen, Molecular Probes
Goat-anti-rabbit Antibody, 488	Invitrogen, Molecular Probes

Table IV: Prepared solutions

Name of prepared solutions	Components
Blocking buffer for western blot	5% milk powder in TBST
Blocking solution for immunofluorescence staining	3% goat serum and 0.05% saponin in PBS
Cytosolic extraction buffer (CEB)	20 mM HEPES [pH 7.2], 250 mM Sucrose, 10 mM KCl, 1.5 mM MgCl ₂ , 2 mM EDTA
Complete cytosolic extraction buffer (CCEB)	CEB with 100 μM PMSF, 1 mM DTT, 0.1% protease inhibitor cocktail

Lysis buffer	50 mM Tris [pH 7.4], 150 mM NaCl, 10% Glycerol, 1% Triton X-100, 2 mM EDTA, 10 mM NaPyrophosphate, 50 mM NaF, 200 μ M Na ₃ VO ₄
TBS (10X)	0.20 M Tris, 1.50 M NaCl [pH 7.6]
TBST	0.1% Tween20 in TBS
Transfer buffer (10X)	0.25 M Tris, 1.87 M Glycine
Transfer buffer	20% MeOH in 1X Transfer buffer

3.2 Methods

3.2.1 Cell culture

In master thesis, three cell lines were used as models to characterize the autophagy-related protein, ATG12 (Table V).

Table V: Cultured cell lines that are used for experiments.

Cell type	Cancer type	Media	Growing type
H1299	Lung	RPMI Medium 1640 + GlutaMAX	Adherent
HCT116	Colon	McCoy's 5A + GlutaMAX (Modified Medium)	Adherent
MDA-MA-231	Breast	DMEM + GlutaMAX (Dulbecco's Modified Eagle Medium)	Adherent

3.2.1.1 Cell passaging

Passaging involves splitting cells and transferring a small number of cells into new flasks. For adherent cultures, cells first need to be detached with trypsin-EDTA. A small number of detached cells can then be used to expand a new culture, while the rest is discarded.

Adherent cells are grown in culture flasks or dishes with the corresponding culture media (Table V), containing 10% FCS and 1% P/S (10 000 units/mL of penicillin and 10 000 µg/mL of streptomycin) at 37°C with 5% CO₂.

The media is removed and cells are washed with PBS. Then 0.5 mL (for small flask) / 1 mL (for middle flask) / 2 mL (for big flask) of trypsin are added to the flask. It is incubated at 37°C for 5 min to get the cells detached from the flask.

To resuspend cells, 4.5 mL (for small flask) / 9 mL (for middle flask) / 18 mL (for big flask) of fresh media is added to the flask with detached cells. Cells should be resuspended by pipetting up and down. An appropriate number of cells is then transferred to new pre-labeled flasks, already filled with fresh media. The new flasks are incubated for the next growth phase. Cells are harvested in a log phase of growth (more than 10%, but less than 100% confluency).

3.2.1.2 Cell freezing

Cells are detached from the culture flask following the procedure for cell passaging. Resuspended cells are transferred to a 15 mL falcon tube. They are centrifuged at 1400 rpm for 5 min. After centrifugation the supernatant is carefully removed without touching the cell pellet. Cell pellet is resuspended in 900 µL FCS and transferred to the pre-labeled cryotube. Then 100 µL DMSO is added and it is mixed well with the cells to maintain a homogeneous cell suspension. The tube is closed and placed in a chamber containing isopropanol and stored at -80°C overnight. Later, vials are transferred to liquid nitrogen tank for indefinite storage.

3.2.1.3 Cell thawing

Vials containing frozen cells are removed from liquid nitrogen tank and held in 37°C water bath to allow rapid thawing of the cells. Meanwhile, 9 mL media is added to a 15 mL falcon tube. Then 1 mL of cells from the vial is transferred to this falcon tube. The cells are

shortly mixed with the pipette and then centrifuged at 1400 rpm for 5 min at RT. After centrifugation supernatant is removed. One milliliter of fresh media is added to the cell pellet and it is resuspended by pipetting. Then all the cells are transferred to the new pre-labeled flask, filled with fresh media. The flask is incubated at 37°C with 5% CO₂ for further culture.

3.2.2 Infecting cells with virus

We used shRNA of ATG12 to produce a virus-mediated transfection system. T293 cells were transfected with plasmid together with the envelope protein vector pMD2G and the packaging vector psPAX2 with the calcium phosphate transfection method. The supernatants are collected after 24 h, filtered through a 0.22 µm filter and stored at -80°C before use.

Cells are seeded in a flask or a 6-well plate. On the day of infection, cell confluence should be more than 70%.

The virus stored at -80°C should be thawed before use. Polybrene is added to the virus in the ratio of 1:100 to increase the efficiency of infection. Then the media is removed from the flask or the plate and virus with polybrene is added (4 mL to the small flask, 2 mL to the well of a 6-well plate). Virus infected cells are cultured for 24 h before replacing the fresh media.

3.2.3 Preparing cell lysate

Cells are detached from the culture flask following the procedure for cell passaging. Resuspended cells are transferred to a 15 mL falcon tube. They are centrifuged at 1400 rpm for 5 min. After centrifugation cells are put on ice and the supernatant is removed. To each cell pellet, 500 µL of cold PBS with protease inhibitor cocktail (in the ratio of 1:1000) is added. Cell pellet is resuspended by pipetting up and down and cells are transferred into pre-labeled eppendorf tubes. Cells are washed once by centrifugation at 1400 rpm for 5 min.

Then all the supernatant is carefully removed without touching the cell pellet. Depending on the size of the pellet, the appropriate amount of lysis buffer is added (20-60 μL depending on the size of the pellet). Lysis buffer is prepared freshly by adding PMSF (0.4 mM) and protease inhibitor cocktail (in the ratio of 1:1000) right before using it.

Cell pellet is resuspended by pipetting and shortly vortexing, so that the cells are mixed well with the lysis buffer. They are left on ice for 15 min and again shortly vortexed before stored at -20°C .

3.2.4 Measuring the protein concentration

BCA Protein Assay is used to measure total protein concentration compared to a protein standard by measuring the absorbance at 562 nm as described in the introduction of this kit.

Lysed samples are taken from the freezer at -20°C and put on ice for 10 min to thaw. They are centrifuged at 13 300 rpm for 10 min at 4°C . Meanwhile, a mixture of reagent A and B in the ratio of 50:1 is prepared. The mixture becomes bright green. After centrifugation the supernatant is transferred in new pre-labeled eppendorf tubes on ice. For measuring the protein concentration, the lysate is diluted 1:10 in distilled water. Eight BSA standards are made by diluting 2 $\mu\text{g}/\mu\text{L}$ albumin standard in distilled water.

Twenty-five microliters of prepared standard and sample is pipetted into appropriate wells of a 96-well plate, each in duplicate. Then 200 μL of prepared reagent A and B is added to each well. Plate is incubated for 5 min at 37°C and then read in a SpectraMax M2 machine at 540 nm. The protein concentration for each cell lysate sample is determined.

3.2.5 Western Blotting

From the measured protein concentrations the exact volumes of lysate, distilled water, loading buffer 4X and DTT 10X are calculated and mixed in an eppendorf tube. The amount of loaded protein varies with the experiment; it is usually between 30-50 μg per sample. Loading volume is 20-30 μL . To denature the samples, they are boiled at 90°C for 5 min and then cooled down to RT. Later they are centrifuged at 13 000 rpm for 3 min.

Chamber for electrophoresis is prepared by inserting the 12% SDS-PAGE gel and filling with running buffer (Table IV). Wells of the gel are washed with running buffer by

pipetting. Equal amounts of protein are put into the wells of the gel, along with molecular weight markers. The gel is run for 30 min at 80 V, followed by 1 h at 135 V until the blue marker goes to the end of the gel.

Meanwhile the transfer buffer is prepared (Table IV). It is cooled at 4°C together with the cassette holder, 5-6 sponges, 2 filters and a polyvinylidene difluoride (PVDF) membrane. The membrane is activated by rinsing it in methanol for 1 min before putting it into transfer buffer. When electrophoresis is finished and the proteins are separated, they must be transferred from the gel to the membrane. The gel is removed from the electrophoresis chamber. Then the transfer stack is prepared. On the back side of the cassette holder 2-3 sponges are laid, followed by the Whatmann paper, the gel, the membrane, again the Whatmann paper and 2-3 sponges. In the stack there should be no bubbles.

The running buffer is replaced by the transfer buffer. Transferring step lasts for 1 h at 30 V for 1 gel or 60 V for 2 gels at 4°C. After transfer, the membrane is rinsed in tap water and then markers are labeled with pen. The membrane is first put in tap water for 5 min, shaking and later in blocking buffer (Table IV) for 1 h with shaking. Blocking the membrane prevents non-specific binding of proteins. The membrane is incubated in appropriate dilution of primary antibody in blocking buffer overnight on rotor at 4°C.

Then the membrane is washed three times with TBST, 7 min each. It is incubated with the HRP-conjugated secondary antibody in blocking buffer (1:3000) at RT for 1 h. Later it is again washed three times with TBST, 7 min each.

The chemiluminescent substrate (ECL, ECL Plus or Luminata Forte) is used for the detection of horseradish peroxidase;

- ECL: the substrate working solution is prepared by mixing Substrate A and Substrate B in a ratio of 1:1
- ECL Plus: the substrate working solution is prepared by mixing Substrate A and Substrate B in a ratio of 40:1
- Luminata forte: ready to use.

The membrane is incubated with 2 mL of working solution for 5 min at RT. Then the membrane is removed from working solution and placed in a film cassette with the protein side facing up. It is covered with transparent plastic wrap and transported to the darkroom.

All lights are turned off except those appropriate for exposure. The film is carefully placed on top of the membrane. The exposure time is adjusted to achieve optimal results. Light emission is most intense during the first 5-30 min after substrate incubation. Film is developed after placing it in the input tray of the X-Omat 2000 processor. Once processing is completed, the machine deposits the film on the outlet tray. After film exposure the membrane is washed in TBST once for 5 min. It is incubated for 30 min at 50°C in stripping buffer, shaking. After washing in TBST for 5 min it is ready to be reused.

3.2.6 Immunofluorescence staining

Cells are grown in a 24-well plate on coverslips. They are cultured in nutrient-rich medium or incubated in starvation conditions in the absence or presence of chloroquine. Cells are incubated at 37°C with 5% CO₂ for the specified time period.

The cells are thereafter washed with 300 µL of PBS at RT for 1-3 min, fixed with 4% PFA for 10 min at RT and further washed with PBS twice. Membrane permeabilization is assessed by treating cells with 0.05% saponin for 5 min. Coverslips are washed with PBS for 3 min, transferred into a ceramic plate where they are covered with acetone, the additional fixative and incubated at -20°C for 10 min. It is advised to remove as much PBS as possible before dropping the coverslip into the acetone.

Coverslips are transferred back in the 24-well plate and they are washed with PBS twice. The coverslips are transferred into the humidified chamber and 60 µL of blocking solution (Table IV) is applied on each of them. They are incubated with blocking solution at RT for 1 h.

After the blocking step, the blocking solution is removed from the coverslips with a pipette. Primary antibodies are diluted in blocking solution and applied to the corresponding coverslips. They are incubated at 4°C overnight.

Coverslips are transferred back in the 24-well plate where they are washed with PBS twice. They are transferred into the chamber and 60 µL of secondary antibodies, diluted in 3.5% BSA, is applied on each of them. They are incubated at RT for 1 h. The choice of secondary antibody is dependent on the donor species of the primary antibody and the desired fluorochrome. Later the coverslips are transferred back in the 24-well plate and washed with PBS two times, 5 min each wash. Each coverslip is inverted onto a cytoslide,

containing 4 μL of mounting media. When mounting media is dried, the coverslips are sealed with nail polish and put at 4°C until microscopy.

Mitotracker (in the ratio of 1:1000 in corresponding media) is added to the treated cells before fixing them with 4% PFA. It is incubated for 20 min at 37°C. When the incubation time is finished, the cells are washed with 300 μL of PBS per well for 1-3 min at RT and fixed with 4% PFA for 10 min at 37°C. The cells are then ready for the immunofluorescence staining as described above, if a co-staining of Mitotracker and protein of interest is desired.

3.2.7 Subcellular fractionation

Cells are grown in a culture flask; at least 10 mio cells are required.

- Cell counting

Cells are detached from the culture flask following the procedure for cell passaging. Resuspended cells in culture medium are transferred to a falcon tube and centrifuged at 1400 rpm for 5 min. The supernatant is removed and the cell pellet is resuspended in 1 mL of media. Cells are needed to obtain an uniform suspension. Neubauer chamber is prepared by placing a coverslip in the middle of that chamber. Ten microliters of the cells, which are diluted 1:100, are transferred to the edge of the Neubauer counting chamber. A droplet of the suspension is expelled and drawn under the coverslip by capillary action. The chamber is placed in the microscope under 10 \times objectives. Cells are counted in each of the four corner squares. Cells overlapping the top and left lines are included in counting but not those overlapping the bottom or right lines (this eliminates redundant counting if adjacent regions are counted).

Cells per milliliter are determined by the following calculations:

$$\text{Cells/mL} = \text{average count per square} \times \text{dilution factor} \times 10^4$$

- Subcellular fractionation

Equal amount of cells are taken from different falcon tubes. They are transferred to an eppendorf tube and centrifuged at 1400 rpm for 5 min. The supernatant is removed and the cell pellet is washed with 1 mL of PBS, containing 0.4% BSA. All the supernatant is

carefully removed. One hundred microliters of complete CEB buffer (Table IV) with digitonin (0.625 mg/mL) are added to the pellet, resuspended and lysed for 10-20 min on ice.

Meanwhile, 5 μ L cells and 5 μ L of Trypan blue solution are mixed in an eppendorf tube, put on a cytoslide and covered with coverslip. The percentage of permeabilized cells is estimated after observing the cytoslide under the microscope (permeabilized cells take up the dye and they are stained blue). When most of the cells are permeabilized (more than 80%), the experiment is continued.

Lysed cells are centrifuged at 700g for 10 min at 4°C. The pellet consists of nuclei and it is discarded. Supernatant is centrifuged at 7000g for 30 min at 4°C. The supernatant is kept on ice until ultracentrifugation. The pellet from the second centrifugation is the mitochondrial fraction. It is washed two times with 500 μ L of cold PBS (the pellet is centrifuged at 1400 rpm for 5 min at 4°C). Then the cell pellet is lysed with 100 μ L of CCEB buffer containing 1% SDS by boiling at 95°C for 5 min. The lysate is centrifuged at 14 000 rpm for 3 min at 4°C. For western blot 19.5 μ L of supernatant is used and the rest is frozen at -20°C.

The supernatant from the second centrifugation is ultracentrifuged at 21 000g for 60 min at 4°C. The pellet consists of lysosomes and peroxisomes. It is lysed with 50 μ L of CCEB buffer containing 1% SDS by boiling at 95°C for 5 min. The lysate is centrifuged at 14 000 rpm for 3 min at 4°C. For western blot 19.5 μ L of supernatant is used and the rest is frozen at -20°C. The supernatant from this centrifugation is the cytosol. For western blot 10 μ L of cytosol is used and the rest is frozen at -20°C.

3.2.8 Quantification of the results

3.2.8.1 Quantification of protein expression on Western Blot

- When detection of the proteins is done by chemiluminescence, films are scanned and bands are analyzed by using the software ImageJ 1.47v (public domain). Each band is quantified by the software and then normalized to the value of its corresponding band of GAPDH.

- When the image is acquired by detecting fluorescence, using Odyssey Fc machine, the bands are quantified with the software Image Studio Ver 3.1 (LI-COR Biosciences) and then normalized to the value of the corresponding band of GAPDH.

3.2.8.2 Colocalization analysis

Images, taken by confocal microscope, are analyzed with the software Imaris 7.5.0 (Bitplane). It measures the correlation of intensity distribution between two channels. One of the coefficients to evaluate the colocalization of two variables, is Pearson's correlation coefficient (R), measuring the linear correlation. The R values vary between -1 and 1. A result of -1 means there is a perfect negative correlation between the two values, while a result of 1 means there is a perfect positive correlation between the two variables. A result of 0 means there is no linear relationship between the two variables. Values close to 1 or -1 indicate a possible correlation between the two variables.

3.2.8.3 Measuring mitochondrial area per cell

Images, taken by confocal microscope are analyzed with the Image-Pro Plus software (MediaCybernetics). The area of mitochondria in one image was selected and calculated by the software. Cell number was counted by selecting the nuclear. The area of mitochondria per cell is then calculated by dividing the total area of mitochondria in one image by the cell number.

4. RESULTS

4.1 ATG12 expression was reduced upon induction of autophagy by starvation.

We were studying the expression of ATG12 after induction of autophagy in tumor cells by performing immunoblotting and immunofluorescence staining.

First, we investigated the expression of proteins ATG1, ATG7, p62, ATG12, ATG5 and GAPDH by immunoblotting. Human colon cancer HCT116 cells, lung cancer H1299 cells and breast cancer MDA-MA-231 cells were left untreated or treated with starvation medium or rapamycin to induce autophagy in the presence or absence of chloroquine (CQ). CQ inhibits degradation of autolysosomes and helps to assess the presence of induced autophagy (38). Relative expression of investigated proteins was quantified by measuring the intensity of bands, relative to the house-keeping protein, GAPDH. It serves as a control to ensure the same total amount of proteins in each sample. Our method for monitoring the autophagic pathway was through observing levels of p62, which is regarded as a selective substrate for autophagy (19). As levels of p62 decreased after starvation and increased after treatment with CQ in starvation media in HCT116 and H1299 cells, we suggest the induction of autophagy (Figure 5). Since we were not able to detect reduced p62 levels after treating MDA-MA-231 cells with starvation media, we cannot assure that the autophagic process was induced (Figure 5).

After treating cells with starvation media we did not observe evident changes of ATG7 and ATG5, whereas the level of ATG12 was decreased (Figure 5). The weakest reduction of ATG12 after starvation was observed in MDA-MA-231 cell line (Figure 5). As known, ATG12 exists in single and conjugated forms, therefore we can detect two bands at different molecular weights by immunoblotting (49). We were able to observe only ATG12 in a conjugate with ATG5 (Figure 5). Detection of ATG1 was successful in MDA-MA-231 cells only, in which the protein levels of ATG1 did not change upon treatment with starvation media or starvation media with CQ (Figure 5).

We also noted that the expression levels of ATG7, p62, ATG12 and ATG5 vary among studied cell lines, suggesting different basal levels of autophagy in these proteins (Figure 5). Next, with anti-ATG12 antibody we detected two bands in HCT116 cell line, among

which the upper band appeared to be more intensive, while in H1299 and MDA-MA-231 cell lines only one band was detected (Figure 5).

Further we investigated the expression of ATG12 in human colon cancer HCT116 cells by performing an immunocytochemistry fluorescence staining. Cells were grown on coverslips and treated under control conditions, starvation-induced autophagy, CQ in culture media and CQ in starvation media. We stained ATG12 and LC3 by using anti-ATG12 and anti-LC3 antibodies. LC3 is widely applied marker for monitoring autophagy since levels of lipidated LC3 correlate with the amount of autophagosomes (38).

Stained microscopic preparates were analyzed under confocal laser scanning microscope, which has the ability to obtain images of thin sample sections at selected depth of the sample (61). We found that LC3 was increased with a punctate pattern after starvation (Figure 6), suggesting formation of autophagosomes and induction of autophagy. Still, we cannot be certain whether increased amount of autophagosomes demonstrates enhanced synthesis or inhibited degradation of double-membrane vesicles. Thus, we use the lysosomal protease inhibitor, such as CQ and compare levels of LC3 in the presence and absence of the applied substance (38, 41). We determined increased LC3 after treatment with CQ in comparison to culture and starvation media itself, indicating induced autophagic process (Figure 6). Interestingly, we observed decreased ATG12 staining after starvation, correlating with the results from immunoblotting. In addition, ATG12 was slightly increased after treatment with CQ and obviously decreased after treatment with CQ in starvation media (Figure 6). Yet, we do not have proper explanation, how CQ affects ATG12 levels.

We observed morphological changes of cells after starvation. Cytoplasm was shrunk and the shape of the cells rounded up (Figure 6).

From the confocal images we compared localization of proteins ATG12 and LC3. As a statistic for measuring colocalization we used Pearson's correlation coefficient (R). It was calculated by software and expressed as the relationship between intensities of each fluorescence channel. For each condition we examined three images, calculating a mean value of Pearson's correlation coefficient (R) and standard deviation with 95% confidence interval. Cell number per image was approximately 17 for cells, grown in culture media and approximately 5 for cells, grown in starvation media.

From measured coefficients $R_{\text{control}} = 0.230 \pm 0.068$, $R_{\text{starvation}} = 0.284 \pm 0.079$, $R_{\text{CQ}} = 0.079 \pm 0.055$ and $R_{\text{starvation\&CQ}} = 0.258 \pm 0.173$ we determined low colocalization of ATG12 and LC3 (Figure 6). LC3 is known to be present on phagophores and completed autophagosomes, while ATG12 associates with autophagosome precursors (35). We suggest that few colocalized puncta of ATG12 and LC3 represent nascent autophagosomal membrane, whereas the majority of ATG12 does not colocalize with LC3 and reveals an interesting staining pattern.

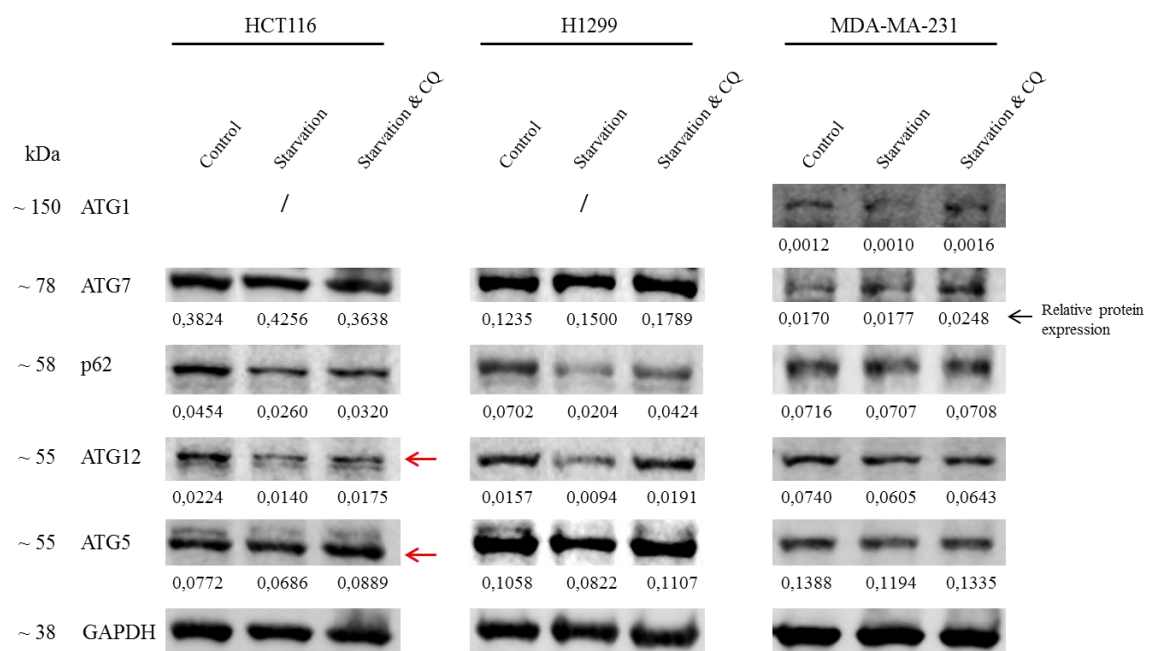


Figure 5: Levels of autophagy-related proteins after induction of autophagy. In corresponding media at 37°C were cultured colon cancer HCT116 and breast cancer MDA-MA-231 cells for 0.5 h, and lung cancer H1299 cells for 2 h. Cell lysates were collected for western blot. 50 µg of protein for each sample was applied on 12% SDS-PAGE gel. Proteins were transferred to a polyvinylidene difluoride membrane and blotted with anti-ATG1 (1:1000), anti-ATG7 (1:1000), anti-p62 (1:1000), anti-ATG12 (1:1000), anti-ATG5 (1:1000) and anti-GAPDH (1:10 000) antibodies. Proteins were identified with fluorophore-conjugated secondary antibodies and detected by fluorescence-based detecting system, Odyssey Fc machine. Quantification of each band was done with the Image Studio Ver 3.1 software. Values of ATG1, ATG7, p62, ATG12 and ATG5 were normalized to the corresponding values of GAPDH.

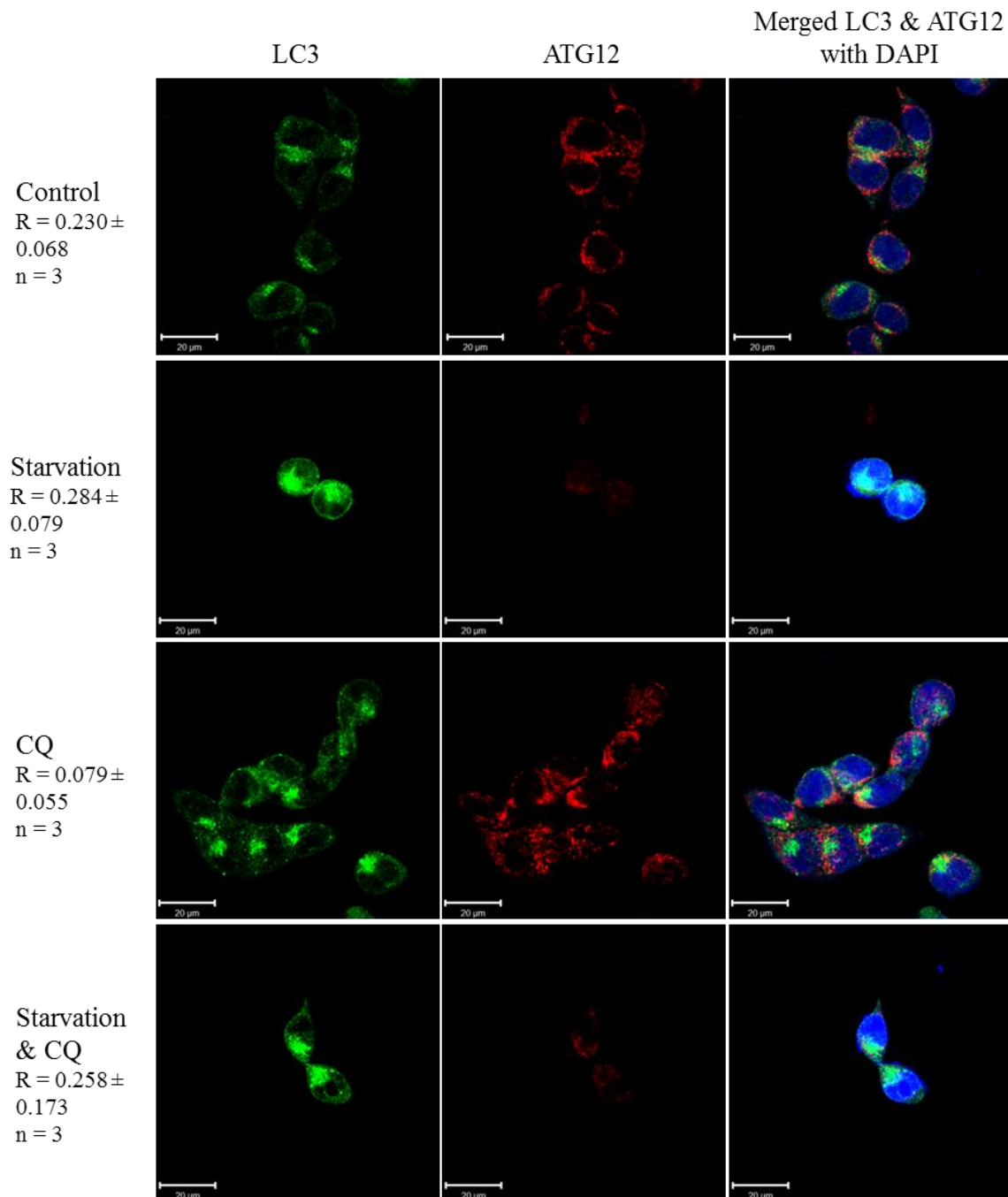


Figure 6: ATG12 was not colocalized with LC3. Colon cancer HCT116 cells were seeded on coverslips and treated with culture media, starvation media, CQ (10 μ M) in culture media or CQ (10 μ M) in starvation media for 1 h at 37°C. The procedure was continued by the immunofluorescence staining, adding mouse anti-ATG12 (1:100) and rabbit anti-LC3 (1:100) antibodies. After examining stained cells under LSM confocal microscope, they were analyzed with the Imaris x64 7.5.0 software, which quantified the colocalization between ATG12 and LC3, presented as Pearson's correlation coefficient (R). Scale: 20 μ m.

4.2 ATG12 was localized on mitochondria.

Further, we were intrigued by the staining pattern of ATG12, which was not typical for an autophagy-related protein. We studied the subcellular location of ATG12 in colon cancer HCT116, lung cancer H1299 and breast cancer MDA-MA-231 cells. We performed immunofluorescence staining using organelle-specific markers: Mitotracker for mitochondria, LysoTracker for lysosomes, ER-tracker for endoplasmic reticulum and Phalloidin for actin filaments. ATG12 was detected applying anti-ATG12 antibody. Colocalization of ATG12 was confirmed with Mitotracker upon considerably high values of Pearson's correlation coefficient ($R_{\text{HCT116}} = 0.653 \pm 0.043$, $R_{\text{MDA-MA-231}} = 0.661 \pm 0.045$, $R_{\text{H1299}} = 0.849 \pm 0.040$) (Figure 7), suggesting colocalization of ATG12 and mitochondria.

In addition, we investigated localization of ATG12 by immunofluorescence staining of ATG12 and mitochondria. ATG12 was co-stained with a specific mitochondrial protein recognized by anti-mitochondria (MTC) antibody (62). Results showed colocalization between stained proteins ($R = 0.514 \pm 0.031$), indicating that in colon cancer HCT116 cells ATG12 might be localized on mitochondria (Figure 8). Dots of ATG12 were visible less clearly in comparison to previous ATG12 staining, seemingly due to application of another anti-ATG12 antibody.

Furthermore, we stained mitochondria and LC3 in colon cancer HCT116, lung cancer H1299 and breast cancer MDA-MA-231 cell lines with Mitotracker and anti-LC3 antibody. The staining pattern of Mitotracker differed from that of LC3. As expected, the Pearson's correlation coefficient showed a low correlation between Mitotracker and LC3 ($R_{\text{HCT116}} = 0.191 \pm 0.087$, $R_{\text{MDA-MA-231}} = 0.130 \pm 0.093$, $R_{\text{H1299}} = 0.307 \pm 0.108$), suggesting that LC3 was not located on mitochondria (Figure 9).

We compared Pearson's correlation coefficients between Mitotracker and ATG12 to those between Mitotracker and LC3. The difference between the values was significant, $p < 0.0001$ (Figure 10) in each studied cell line, including colon cancer HCT116, lung cancer H1299 and breast cancer MDA-MA-231 cell lines. The majority of ATG12 puncta did not colocalize with LC3 on phagophores but with mitochondrial marker, proposing mitochondrial localization of ATG12.

Further, we investigated colocalization of ATG12 and ATG5 in breast cancer MDA-MA-231 cells. Autophagy-related proteins were stained using anti-ATG12 and anti-ATG5 antibodies. Since ATG12 and ATG5 form a conjugate during autophagy (3), we expected punctate colocalization of stained proteins on autophagosomal precursors. Surprisingly, the Pearson's correlation coefficient was very low ($R = 0.056 \pm 0.034$), indicating minimal colocalization between ATG5 and ATG12 (Figure 11).

Moreover, we performed subcellular fractionation to separate mitochondrial fraction from the rest of the cell contents. Our purpose was to investigate whether ATG12 can be detected in the mitochondrial fraction. As CQ prevents degradation of autolysosomes (2) it was included in experiment to investigate whether it affects the fractions. Successful separation of mitochondrial, lysosomal and cytosolic fraction in breast cancer MDA-MA-231 cells was determined by detection of different organelle-specific proteins. Lysosomal protein LAMP-1 is recognized by anti-LAMP-1 antibody (63) and its absence in mitochondrial fraction implied efficient fractionation. In addition, anti-mitochondrial (MTC) antibody, bound to a specific mitochondrial protein (62) was observed only in mitochondrial fraction, indicating that entire mitochondria were present in isolated mitochondrial fraction. A cytosolic protein LC3-I was detected only in cytosolic and lysosomal fraction. Additionally, specific autophagosomal marker LC3-II was not present in mitochondrial fraction. Taken together, we assumed the fractionation was sufficiently pure to detect the location of ATG12 (Figure 12). Levels of proteins show moderate changes after treatment with CQ. Yet, we do not have proper explanation for the impact of CQ on protein levels.

However, results showed the presence of ATG12 only in the mitochondrial fraction. Since ATG12 was detected in the same fraction as mitochondrial marker MTC but not in the fraction containing a lysosomal protein LAMP-1 (63), we excluded ATG12 being a part of lysosomes (Figure 12).

The results corresponded to the data of immunofluorescence staining, hence supported our hypothesis that ATG12 might be located on mitochondria (Figure 12).

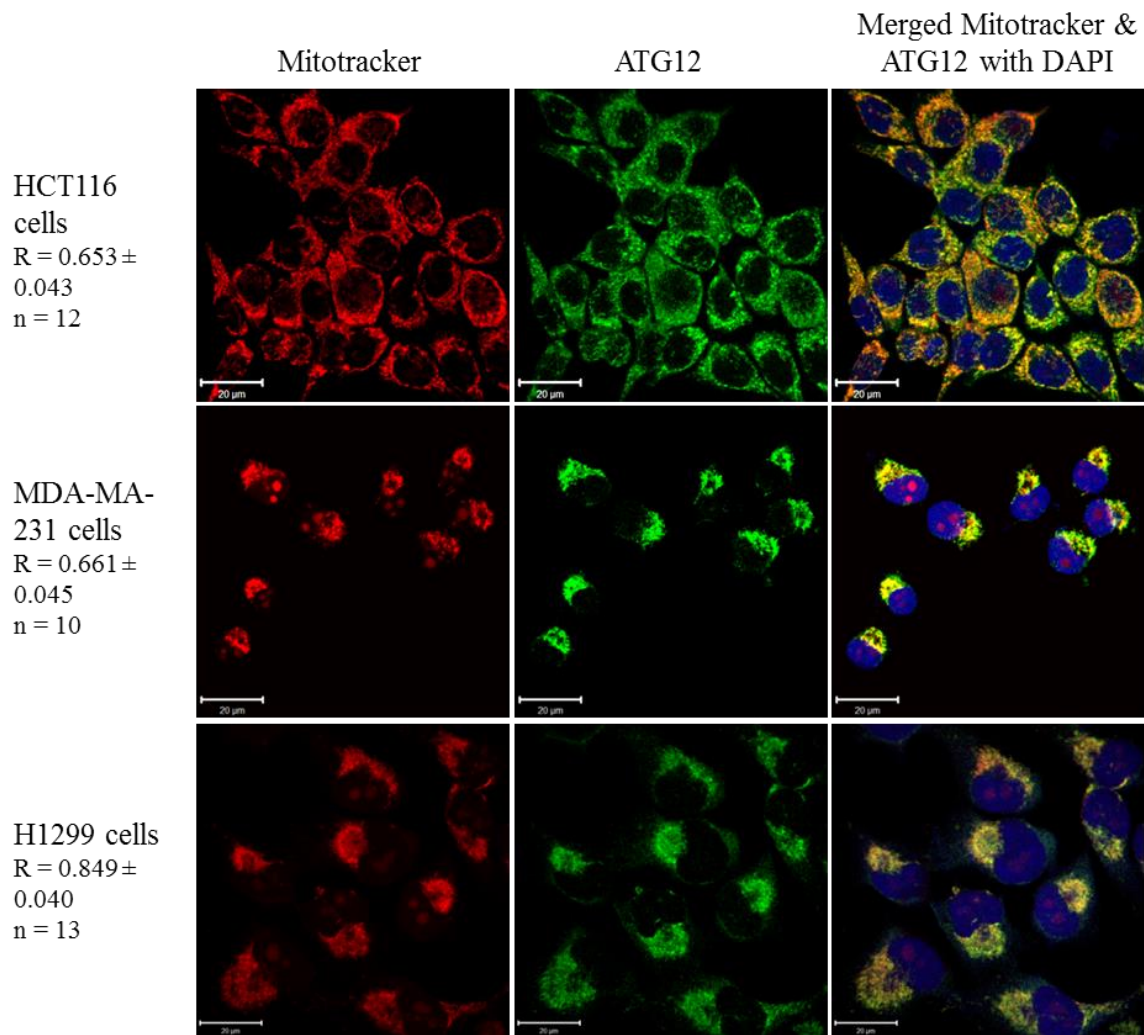


Figure 7: ATG12 was colocalized with Mitotracker. Colon cancer HCT116, breast cancer MDA-MA-231 and lung cancer H1299 cells were seeded on coverslips and incubated at 37°C in culture media until they reached approximately 80% confluence. They were incubated with Mitotracker (1:1000) for 20 min at 37°C, washed with PBS twice and fixed with 4% PFA for 10 min at 37°C. The procedure was followed by the immunofluorescence staining protocol and mouse anti-ATG12 antibody (1:100) was added. Stained cells were examined under LSM confocal microscope and analyzed with the Imaris x64 7.5.0 software to calculate the R values. Scale: 20 μm.

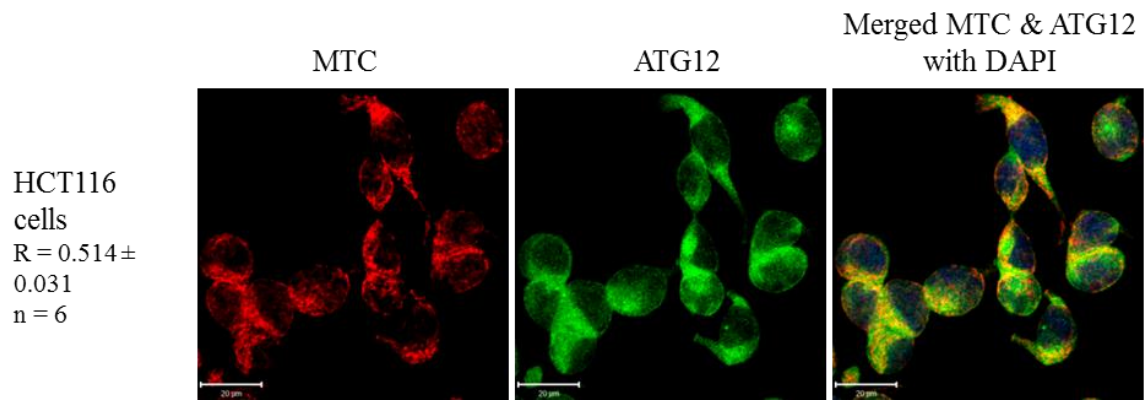


Figure 8: ATG12 was colocalized with MTC. Colon cancer HCT116 cells were seeded on coverslips and incubated at 37°C in culture media until they reached approximately 80% confluence. The procedure was followed by the immunofluorescence staining protocol, adding rabbit anti-ATG12 (1:100) and mouse anti-MTC (1:100) antibodies. After examining stained cells under LSM confocal microscope, they were analyzed with the Imaris x64 7.5.0 software to calculate the R value. Scale: 20 μm.

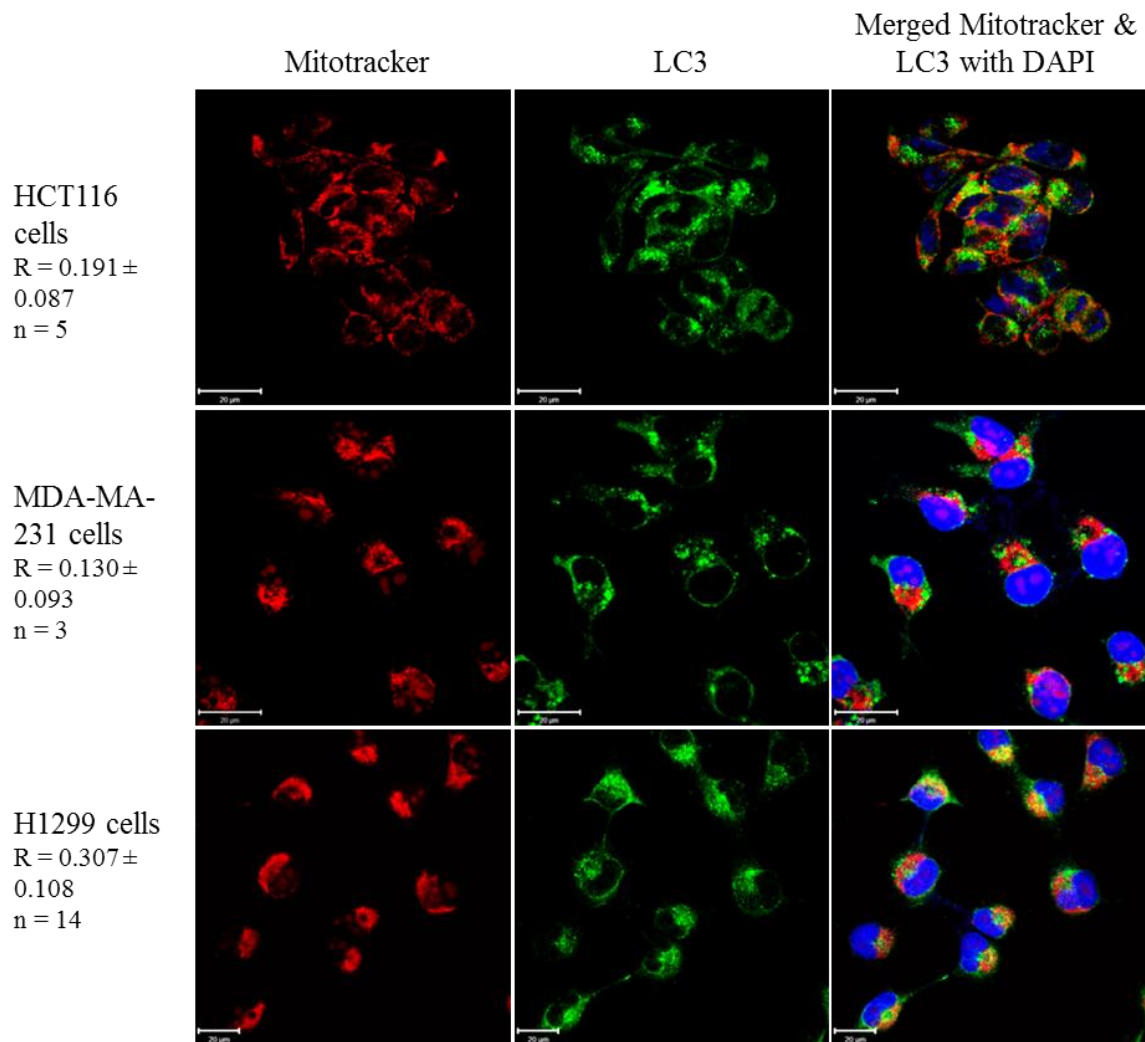


Figure 9: LC3 was not colocalized with Mitotracker. Colon cancer HCT116, breast cancer MDA-MA-231 and lung cancer H1299 cells were seeded on coverslips and incubated at 37°C in culture media until they reached approximately 80% confluence. Cells were incubated with Mitotracker (1:1000) for 20 min at 37°C, with PBS twice and fixed with 4% PFA for 10 min at 37°C. The procedure was followed by the immunofluorescence staining, adding mouse anti-LC3 antibody (1:100). Cells were examined under LSM confocal microscope and analyzed with the Imaris x64 7.5.0 software to calculate the R values. Scale: 20 μm.

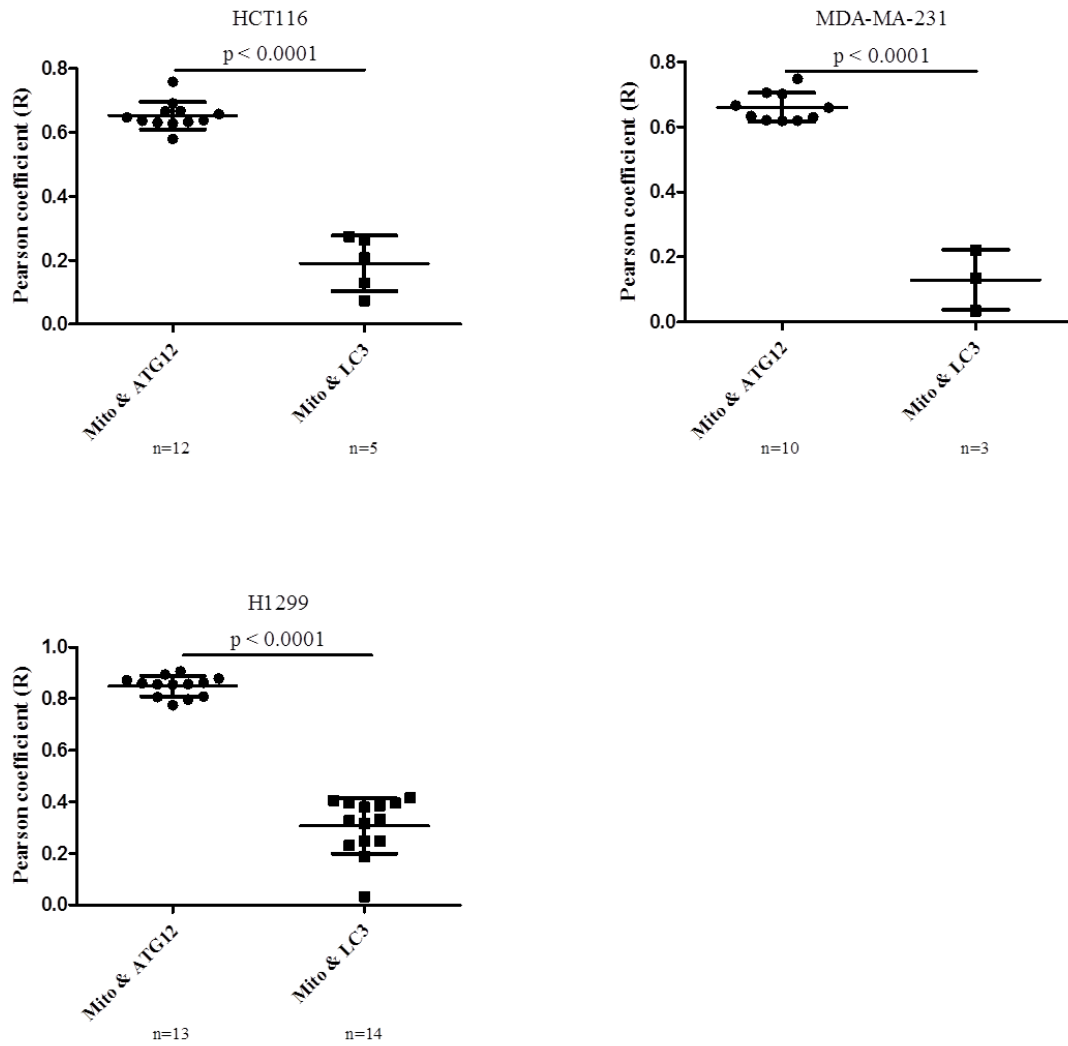


Figure 10: Significant difference between ATG12 staining with Mitotracker and LC3 staining with Mitotracker. Pearson's correlation coefficients (R) of ATG12 staining with Mitotracker were compared to those of LC3 staining with Mitotracker in colon cancer HCT116, breast cancer MDA-MA-231 and lung cancer H1299 cells. The R-values were analyzed with the GraphPad Prism 5. Values were presented as means \pm SDs, from more than three images. The two-tailed p values were obtained using an unpaired Student's *t* test. Values of $p < 0.05$ were considered statistically significant.

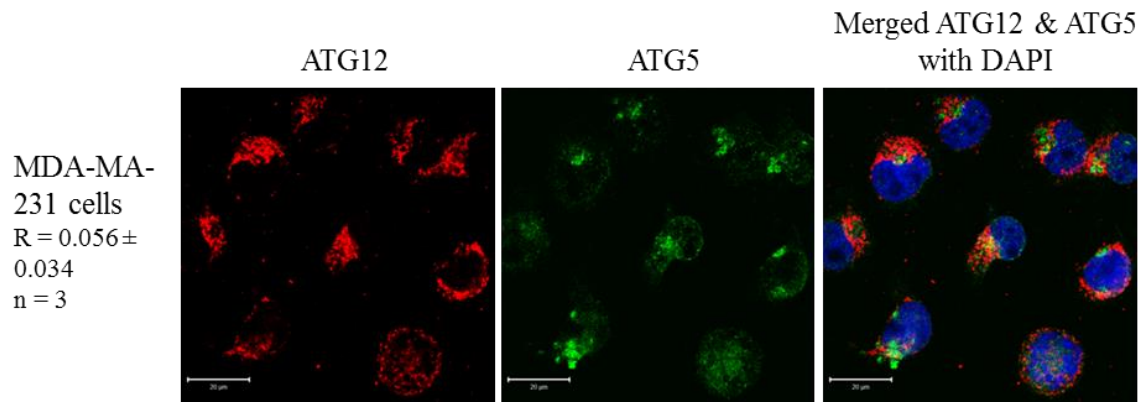


Figure 11: ATG12 was not colocalized with ATG5. Breast cancer MDA-MA-231 cells were seeded on coverslips and incubated at 37°C in culture media until they reached approximately 80% confluence. Procedure was followed by the immunofluorescence staining, adding mouse anti-ATG12 (1:100) and rabbit anti-ATG5 (1:100) antibodies. Stained cells were examined under LSM confocal microscope and analyzed with the Imaris x64 7.5.0 software to calculate the R value. Scale: 20 µm.

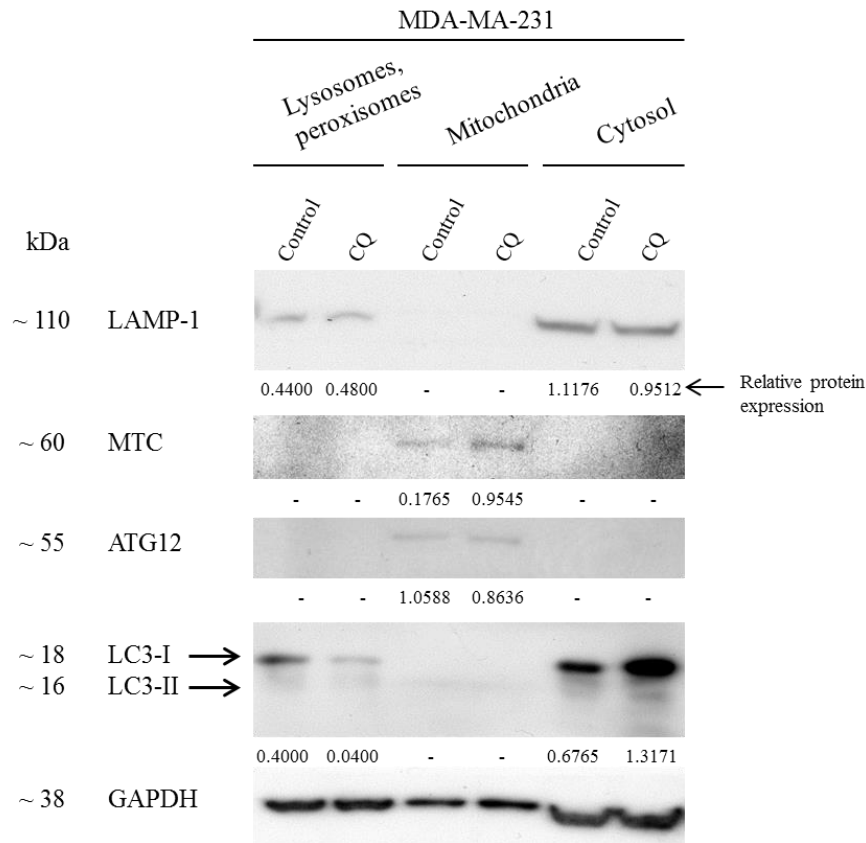


Figure 12: ATG12 was located in mitochondrial fraction. Sixteen millions of breast cancer MDA-MA-231 cells were either untreated or treated with CQ (10 μ M) for 1 h. Subcellular fractionation was performed as described in Materials and Methods. Collected samples were subjected to western blot analysis using anti-ATG12 (1:1000), anti-LAMP-1 (1:1000), anti-MTC (1:1000), anti-LC3 (1:1000) and anti-GAPDH antibodies (1:10 000). Proteins were identified with HRP-linked secondary antibodies and detected by chemiluminescent method, using X-Omat 2000 processor. Isolation of mitochondrial fraction was successfully accomplished, shown by the corresponding fractions of LAMP-1, MTC and LC3.

4.3 Downregulation of ATG12 led to reduced number of mitochondria.

For the purpose of investigating whether ATG12 has an effect on mitochondria, we silenced our gene of interest using RNA interference. It is a process, mediated by small double-stranded RNAs, deriving from virus genome. Small RNAs integrate into the RNA-induced silencing complex (RISC), bind to the complementary sequence of target mRNA and cleave the molecule. Degradation of mRNA and inhibited translation consequently lead to suppressed gene expression (64, 65). We infected breast cancer MDA-MA-231 cells with Lentivirus, containing the construct of shRNA for ATG12. As a negative control we infected cells with empty vector. Successful gene silencing was proven by western blotting, showing the reduction of ATG12 in knockdown cells (Figure 13).

In addition, basal level of autophagy was decreased after knocking down ATG12, shown by increased level of LC3-I and decreased level of LC3-II, displaying reduced ratio of LC3-II to LC3-I. Moreover, in cells with reduction of ATG12, p62 was increased, again indicating a reduction of the basal level of autophagy (Figure 13).

When comparing control cells to the cells with deficient ATG12 expression (shATG12), we noticed morphological changes, which occurred approximately three days after infection. Cells deficient for ATG12 appeared much bigger and flatter, getting slowly detached from the cell flask in contrast to the control cells (Figure 14). After several days, the majority of cells were dead due to their detachment from the flask surface.

Next, we wanted to study whether ATG12 affects the number of mitochondria. Therefore we stained mitochondria with anti-mitochondria (MTC) antibody and compared vector cells with the knockdown cells. From the confocal images we observed that the number of mitochondria in cells with downregulation of ATG12 could be reduced (Figure 15).

To further analyze the impact of reduced ATG12 on mitochondrial number we quantified the average mitochondrial area per cell in confocal images. Values were calculated by software and compared between cells with and without downregulation of ATG12. Results showed that vector cells had significantly larger area of mitochondria ($p = 0.0007$) in comparison to the cells with knockdown of ATG12, suggesting that ATG12 might have an influence on the number of mitochondria (Figure 16).

In addition we stained ATG12 together with Mitotracker as a mitochondrial marker. Successful downregulation of ATG12 was shown by immunofluorescence staining (Figure 17). We observed again decreased number of mitochondria in ATG12 knockdown cells in comparison to the vector cells (Figure 17).

In summary, ATG12 seemed to have an undescribed mitochondrial colocalization and its downregulation led to reduced number of mitochondria.

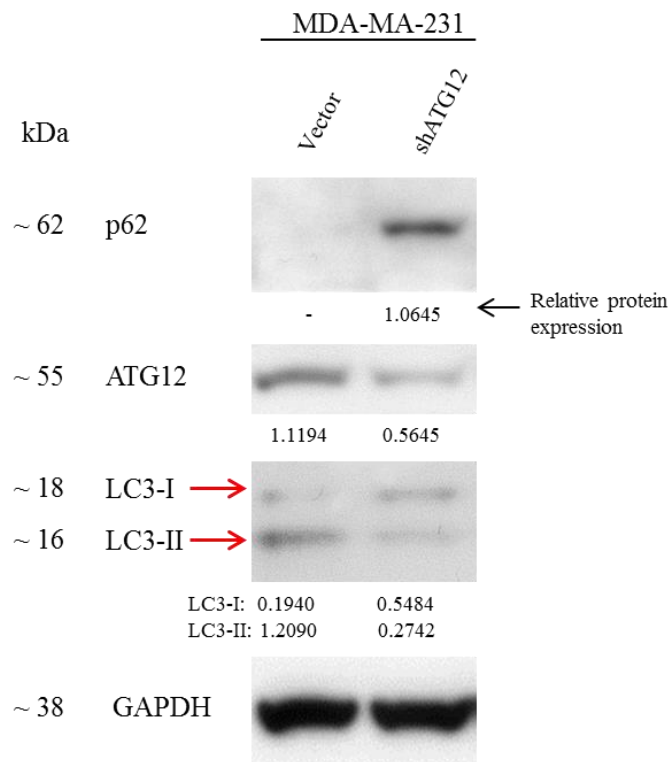


Figure 13: Downregulation of ATG12 by Lentivirus transfection. Breast cancer MDA-MA-231 cells were infected with vector as a negative control and virus to downregulate ATG12. Cells were then lysed and 50 µg of protein for each sample was applied on 12% SDS-PAGE gel. Proteins were transferred to a polyvinylidene difluoride membrane and blotted with anti-ATG12 (1:1000), anti-LC3 (1:1000), anti-p62 (1:1000) and anti-GAPDH (1:10 000) antibodies. Proteins were identified with HRP-linked secondary antibodies and detected by chemiluminescent method, using X-Omat 2000 processor. By reduced ATG12 we observed decreased ratio of LC3-II to LC3-I and increased p62, reflecting the reduced basal level of autophagy.

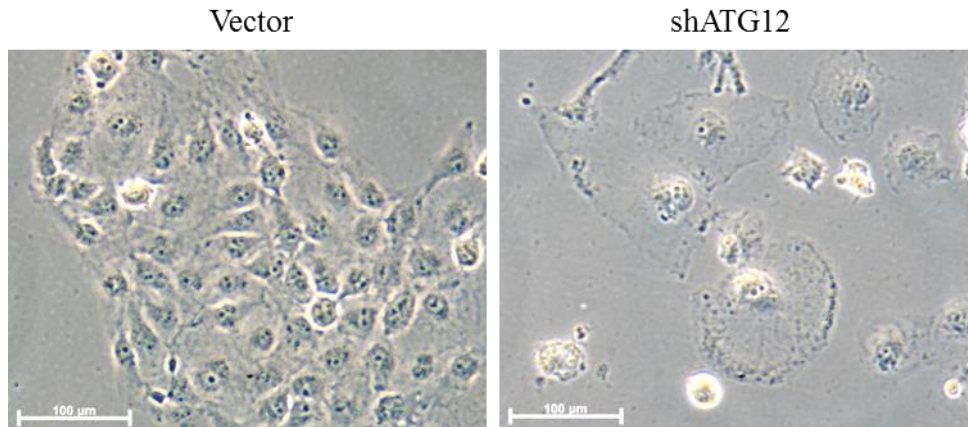


Figure 14: Morphological changes of cells with downregulation of ATG12. Photos were taken with Zeiss Axiovert 35 light microscope, 7 days after infection. Cells with downregulation of ATG12 showed morphological changes in comparison to vector cells. Vector cells had normal shape and size, whereas shATG12 cells were widening, getting bigger and flatter. Scale: 100 µm.

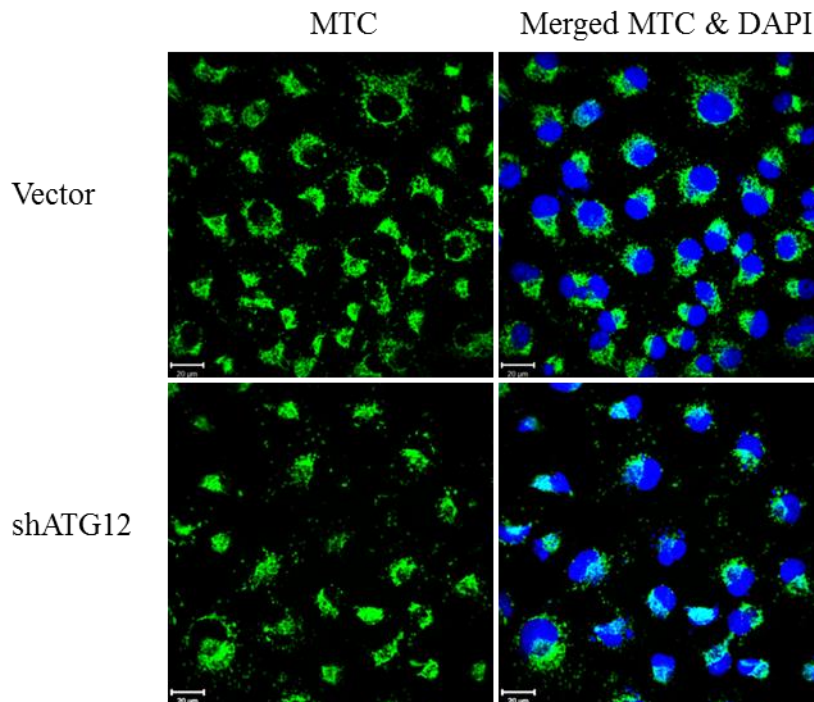


Figure 15: Reduced mitochondrial number in cells with deficient ATG12 expression. Infected breast cancer MDA-MA-231 cells were seeded on coverslips and incubated at 37°C in culture media until they reached approximately 80% confluence. The procedure was followed

by the immunofluorescence staining protocol, adding mouse anti-MTC (1:200) antibody. Stained cells were observed under LSM confocal microscope. Scale: 20 μm .

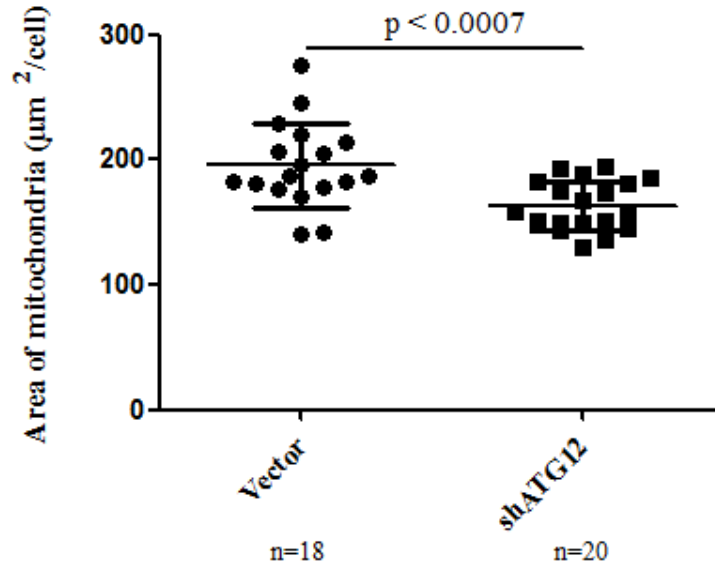


Figure 16: Significantly smaller area of mitochondria in cells with downregulation of ATG12. Confocal microscope was used to take images of vector and shATG12 cells, stained with mouse anti-MTC antibody. 18 images with vector cells and 20 images with shATG12 cells were analyzed by Image Pro Plus software, evaluating mitochondrial area (μm^2 per cell) for each image. The R-values were analyzed with the GraphPad Prism 5. Values were presented as means \pm SDs. The two-tailed p values were obtained using an unpaired Student's *t* test. Values of $p < 0.05$ were considered statistically significant.

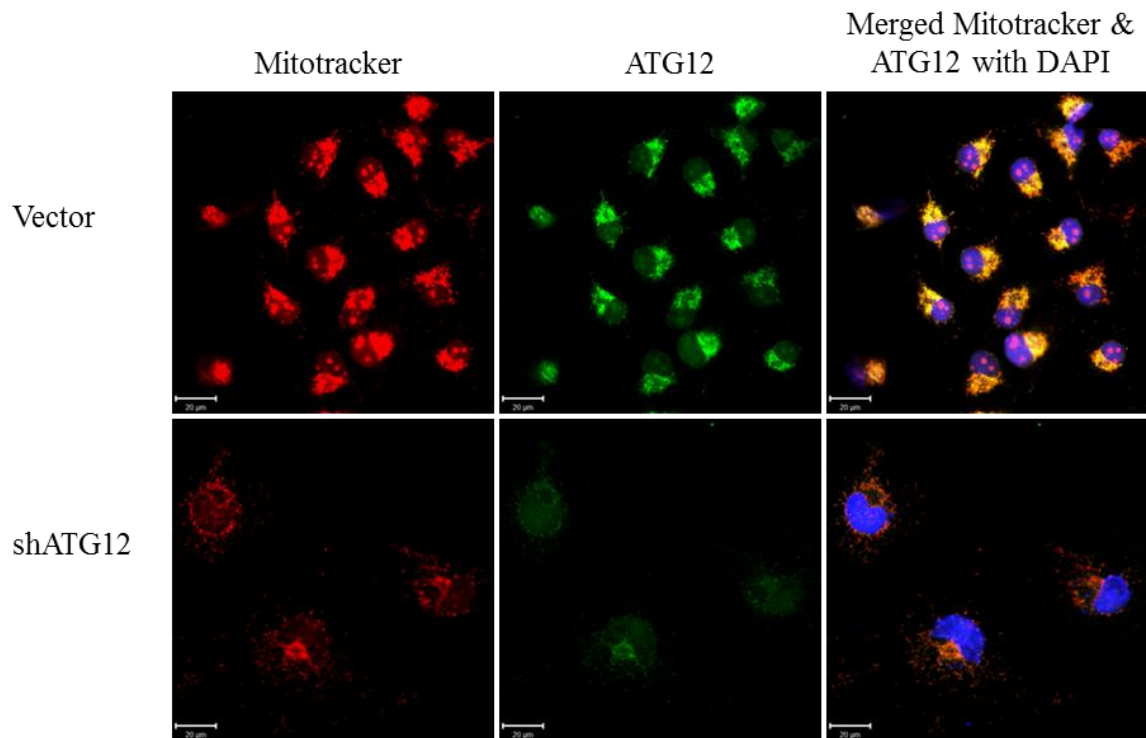


Figure 17: Reduced mitochondrial number in cells with downregulation of ATG12. Colon cancer MDA-MA-231 cells were seeded on coverslips and incubated at 37°C in culture media until they reached approximately 80% confluence. Cells were incubated with Mitotracker (1:1000) for 20 min at 37°C, washed with PBS twice and fixed with 4% PFA for 10 min at 37°C. The procedure was followed by the immunofluorescence staining, adding mouse anti-ATG12 antibody (1:100). Cells were observed under LSM confocal microscope. Staining showed successful downregulation of ATG12 in knockdown cells. Moreover, in ATG12 knockdown cells reduced number of mitochondria was observed. Scale: 20 μm.

5. DISCUSSION

The aim of my thesis was to characterize autophagy-related protein 12 in tumors. We evaluated the effect of autophagy induction on cellular levels of ATG12 in human cancer cells. We determined subcellular localization of ATG12 and elaborated on its function.

First, we demonstrated the reduction of ATG12 after starvation-induced autophagy by immunoblotting. Since we could not detect single ATG12, we observed only ATG12 in a conjugate with ATG5. Single ATG12 might have been present in very small quantities or degraded during lysate preparation.

By using anti-ATG12 or anti-ATG5 antibody for ATG12-ATG5 conjugate detection we observed two bands in colon cancer HCT116 cell line, but only one in lung cancer H1299 and breast cancer MDA-MA-231 cell lines. In HCT116 cells we cannot certainly determine which band represents the specific protein conjugate or which compound is presented by the second band. The presence of protein modifications may also be possible. Since we quantified the expression of each detected protein, we decided that in case of double bands we quantify the more intensive band. We cannot assure whether ATG12 in HCT116 cell line really represents the upper band and whether ATG5 represents the lower one.

After starvation induced autophagy we observed decreased levels of ATG12 while levels of ATG5 show barely visible reduction. With anti-ATG12 and anti-ATG5 antibodies we expect to determine the same ATG12-ATG5 conjugate, therefore protein levels of ATG12 and ATG5 should correlate.

We were able to detect ATG1 in MDA-MA-231 cells, but not in HCT116 and H1299 cell lines. The reason might have been a low ATG1 expression in HCT116 and H1299 cells or the protein degradation during lysate preparation.

We determined the induction of autophagy through decreased levels of p62 after starvation and increased p62 levels after treatment with CQ in starvation media in HCT116 and H1299 cell lines. We did not observe reduced p62 levels after treating MDA-MA-231 cells with starvation media. As the incubation period might have been too short, we suggest performing a time course experiment with MDA-MA-231 cells to find a good time point by which cells response to starvation.

To better estimate the autophagic flux we could also treat cells with CQ in culture media and observe increased p62 levels. Expression of p62 may occasionally change independently of autophagy (41), hence the usage of additional markers for evaluation of autophagy (e.g. LC3) is preferred.

Furthermore, we determined reduced levels of ATG12 after starvation-induced autophagy by immunofluorescence staining as well. In cells, treated with starvation media, the induction of autophagy was suggested after monitoring increased number of LC3 puncta, presenting LC3-II. What is more, we observed elevated LC3 levels in the presence of CQ. Results confirmed that an increase in LC3 levels was rather due to successful enhancement of autophagic flux than to restricted autophagosomal degradation.

Alternatively, we could monitor autophagy after staining p62 with anti-p62 antibody.

The average number of cells, which were grown in culture media, was usually higher in comparison to cells, grown in starvation media. Starved cells were more easily getting detached from the flask surface during washing with PBS, hence they were unintentionally washed away.

Colocalization analysis of ATG12 and LC3 revealed an interesting staining pattern of ATG12, since a great part of ATG12 puncta did not colocalize with LC3 on pre-autophagosomal membranes as expected. We assumed that ATG12 was located on a membrane specific organelle. In addition, we could improve the reliability of results by staining ATG12 and LC3 in lung cancer H1299 cells and breast cancer MDA-MA-231 cells as well.

Values of Pearson's correlation coefficient between ATG12 and mitochondrial markers were considerably high, but not more than 0.849. We suggest that the majority of ATG12 was located on mitochondria, while only few ATG12 puncta were still present on phagophores.

We determined low Pearson's correlation coefficients between LC3 and mitochondrial marker, indicating LC3 was not localized on mitochondria. Still, the values were not less than 0.130. Since LC3 associates with autophagic bodies (35), few colocalized puncta of LC3 and MTC may be observed due to engulfment of damaged or excessive mitochondria by autophagosomes during basal autophagy.

Surprisingly, we observed very low colocalization of ATG12 and ATG5, suggesting detection of very few ATG12-ATG5 conjugates on pre-autophagosomal membranes. In order to support or discard our data, we suggest additional staining of LC3 and ATG5 to provide the evidence about punctate localization of ATG5. It would also be convenient to perform staining of ATG5 and mitochondria.

With the purpose to further investigate the location of ATG12, we performed subcellular fractionation. ATG12 was detected only in mitochondrial fraction, which was correlating with the results from immunofluorescence staining.

Based on the results from immunofluorescence staining and immunoblotting we cannot determine which form of ATG12 is located in the mitochondria. In future research, the proper form of mitochondria localized ATG12 needs to be investigated.

Next, the knockdown of ATG12 expression was successfully performed as we observed downregulation of ATG12. We determined that the reduction of ATG12 affects the basal level of autophagy, which was expectedly decreased in ATG12 knockdown cells. Reduction of ATG12 was sufficiently proven by observing LC3 and p62 markers.

Additionally, we could have examined how are ATG5 levels affected by downregulation of ATG12. Reduced levels of ATG5 in conjugated form would support successful ATG12 reduction since less ATG12 would be available for conjugation with ATG5. Efficient infection might have been proven by immunofluorescence staining of autophagic vacuoles as well, resulting in decreased vesicle staining due to reduced autophagic level in ATG12 knockdown cells. Similarly, we might have stained ATG12 and LC3 to observe their reduction in efficiently infected cells.

Furthermore, we have determined that downregulation of ATG12 results in decreased number of mitochondria, suggesting the impact of ATG12 on mitochondrial biogenesis.

Since we demonstrated the reduction of mitochondria in cells with deficient ATG12 expression, it would be interesting to examine whether upregulation of ATG12 gene expression leads to increased mitochondrial number.

As stated above, our group previously observed the upregulation of ATG12 in several types of solid tumors. Similarly, it was documented that ATG12 was upregulated in breast carcinoma cells, leading to increased autophagy and facilitated resistance to a specific

oncogene-targeted therapy. ATG12 was determined to be upregulated at the transcriptional level due to increased expression of ATG12 mRNA. Next, after knockdown of ATG12 the tumor growth was reduced and drug resistance decreased (66).

Tumors may suffer from insufficient nutrient and oxygen supply owing to their high metabolic rate in comparison to normal tissues (20). In addition to the role of ATG12 in regulating autophagy, it could promote tumor survival by providing sufficient amounts of mitochondria, the main intracellular source of energy (52).

Potential role of ATG12 in mitochondrial growth and functioning is yet not known, therefore, we recommend additional assays to evaluate mitochondrial biogenesis in presence and absence of ATG12. Isolation of genomic DNA is followed by amplification of the specific mitochondrial region, compared with a genomic region by using real-time PCR. Levels of mitochondrial encoded proteins or mitochondrial biogenesis factors can be detected by immunoblotting respectively, e.g. subunits of cytochrome c oxidase and PGC-1 α , master regulator of oxidative phosphorylation (67, 68).

6. CONCLUSION

Mechanism of autophagy and its role in tumorigenesis are very complex, hence compelling for research. In our study, performed on human cancer cell lines, we focused on the characterization of ATG12, an indispensable protein for efficient autophagic process.

Levels of ATG12 were reduced after starvation-induced autophagy in comparison to untreated cells.

We determined colocalization of ATG12 and mitochondrial markers, while minimal colocalization of ATG12 and LC3 or ATG5 was detected.

After knockdown of ATG12 we observed morphological changes and reduced number of mitochondria in infected cells. We suggest that ATG12 might have a positive impact on mitochondrial biogenesis. As ATG12 was observed to be upregulated in several types of solid tumors, it could be able to promote cancer progression by supporting mitochondrial growth.

Further studies will be needed to reveal the role and importance of ATG12 in cancer, particularly to research whether ATG12 might serve as a potential target for cancer treatment.

7. REFERENCES

1. Liu H, He Z, Simon HU: *Targeting autophagy as a potential therapeutic approach for melanoma therapy*. *Seminars in cancer biology* 2013; 23(5): 352-60.
2. Ohsumi Y: *Historical landmarks of autophagy research*. *Cell research* 2014; 24(1): 9-23.
3. Wirawan E, Vanden Berghe T, Lippens S, Agostinis P, Vandenabeele P: *Autophagy: for better or for worse*. *Cell research* 2012; 22(1): 43-61.
4. Wu WKK, Coffelt SB, Cho CH, Wang XJ, Lee CW, Chan FKL, Yu J, Sung JJY: *The autophagic paradox in cancer therapy*. *Oncogene* 2012; 31(8): 939-53.
5. Lamb CA, Yoshimori T, Tooze SA: *The autophagosome: origins unknown, biogenesis complex*. *Nature reviews – Molecular cell biology* 2013; 14(12): 759-74.
6. Alberts B, Bray D, Hopkin K, Johnson A, Lewis J, Raff M, Roberts K, Walter P: *Essential cell biology*. Garland science 2014.
7. Eskelinen EL: *The dual role of autophagy in cancer*. *Current opinion in pharmacology* 2011; 11(4): 294-300.
8. Yang Z, Klionsky DJ: *An overview of the molecular mechanism of autophagy*. *Current topics in microbiology and immunology* 2009; 335: 1-32.
9. Dumont FJ, Su Q: *Mechanism of action of the immunosuppressant rapamycin*. *Life sciences* 1996; 58(5): 373-95.
10. Pan T, Kondo S, Zhu W, Xie W, Jankovic J, Le W: *Neuroprotection of rapamycin in lactacystin-induced neurodegeneration via autophagy enhancement*. *Neurobiology of disease* 2008; 2(1): 16-25.
11. Zhou X, Li C, Lu X: *Autophagy activation by rapamycin improves left ventricular function in diabetic rats*. *International journal of cardiology* 2013; 168(4): 4429-31.
12. Yorimitsu T, Klionsky DJ: *Autophagy: molecular machinery for self-eating*. *Cell death and differentiation* 2005; 12(Suppl 2): 1542-52.

13. Solomon VR, Lee H: *Chloroquine and its analogs: a new promise of an old drug for effective and safe cancer therapies*. European journal of pharmacology 2009; 625(1-3): 220-33.
14. Egger ME, Huang JS, Yin W, McMasters KM, McNally LR: *Inhibition of autophagy with chloroquine is effective in melanoma*. The journal of surgical research 2013; 184(1): 274-81.
15. Kaneko M, Nozawa H, Hiyoshi M, Tada N, Muroto K, Nirei T, Emoto S, Kishikawa J, Iida Y, Sunami E, Tsuno NH, Kitayama J, Takahashi K, Watanabe T: *Temsirolimus and chloroquine cooperatively exhibit a potent antitumor effect against colorectal cancer cells*. Journal of cancer research and clinical oncology 2014; 140(5): 769-81.
16. Myeku N, Figueiredo-Pereira ME: *Dynamics of the degradation of ubiquitinated proteins by proteasomes and autophagy: association with sequestosome 1/p62*. The journal of biological chemistry 2011; 286(25): 22426-40.
17. Bitto A, Lerner CA, Nacarelli T, Crowe E, Torres C, Sell C: *p62/SQSTM1 at the interface of aging, autophagy, and disease*. Age (Dordr) 2014.
18. Ichimura Y, Komatsu M: *Selective degradation of p62 by autophagy*. Seminars in immunopathology 2010; 32(4): 431-6.
19. Bjørkøy G, Lamark T, Pankiv S, Øvervatn A, Brech A, Johansen T: *Monitoring autophagic degradation of p62/SQSTM1*. Methods in enzymology 2009; 452: 181-97.
20. Kimmelman AC: *The dynamic nature of autophagy in cancer*. Genes&development 2011; 25(19): 1999-2010.
21. Chen N, Debnath J: *Autophagy and tumorigenesis*. FEBS letters 2010; 584(7): 1427-35.
22. Tschan MP, Simon HU: *The role of autophagy in anticancer therapy: promises and uncertainties*. Journal of internal medicine 2010; 268(5): 410-8.
23. Liu H, He Z, Simon HU: *Autophagy suppresses melanoma tumorigenesis by inducing senescence*. Autophagy 2014; 10(2): 372-3.

24. Liu H, He Z, von Rütte T, Yousefi S, Hunger RE, Simon HU: *Down-regulation of autophagy-related protein 5 (ATG5) contributes to the pathogenesis of early-stage cutaneous melanoma*. Science translational medicine 2013; 5: 202ra123.
25. DeVita VT Jr, Lawrence TS, Rosenberg SA: *Cancer: Principles & Practice of Oncology - Primer of the Molecular Biology of Cancer*. Lippincott Williams&Wilkins 2011.
26. Janku F, McConkey DJ, Hong DS, Kurzrock R: *Autophagy as a target for anticancer therapy*. Nature reviews - Clinical oncology 2011; 8(9): 528-39.
27. Yang S, Wang X, Contino G, Liesa M, Sahin E, Ying H, Bause A, Li Y, Stommel JM, Dell'antonio G, Mautner J, Tonon G, Haigis M, Shirihai OS, Doglioni C, Bardeesy N, Kimmelman AC: *Pancreatic cancers require autophagy for tumor growth*. Genes&development 2011; 25(7): 717-29.
28. Fernández-Medarde A, Santos E: *Ras in cancer and developmental diseases*. Genes cancer 2011; 2(3): 344-58.
29. Guo JY, Chen HY, Mathew R, Fan J, Strohecker AM, Karsli-Uzunbas G, Kamphorst JJ, Chen G, Lemons JM, Karantza V, Coller HA, Dipaola RS, Gelinas C, Rabinowitz JD, White E: *Activated Ras requires autophagy to maintain oxidative metabolism and tumorigenesis*. Genes&development 2011; 25(5): 460-70.
30. White E: *Deconvoluting the context-dependent role for autophagy in cancer*. Nature reviews - Cancer 2012; 12(6): 401-10.
31. Ma XH, Piao S, Wang D, McAfee QW, Nathanson KL, Lum JJ, Li LZ, Amaravadi RK: *Measurements of tumor cell autophagy predict invasiveness, resistance to chemotherapy, and survival in melanoma*. Clinical cancer research 2011; 17(10): 3478-89.
32. Paoli P, Giannoni E, Chiarugi P: *Anoikis molecular pathways and its role in cancer progression*. Biochimica et biophysica acta 2013; 1833(12): 3481-98.
33. Klionsky DJ et al: *Guidelines for the use and interpretation of assays for monitoring autophagy*. Autophagy 2012; 8(4): 445-544.
34. Eskelinen EL, Reggiori F, Baba M, Kovács AL, Seglen PO: *Seeing is believing: the impact of electron microscopy on autophagy research*. Autophagy 2011; 7(9): 935-56.

35. Klionsky DJ, Cuervo AM, Seglen PO: *Methods for monitoring autophagy from yeast to human*. *Autophagy* 2007; 3(3): 181-206.
36. Shaid S, Brandts CH, Serve H, Dikic I: *Ubiquitination and selective autophagy*. *Cell death differentiation* 2013; 20(1): 21-30.
37. Klionsky D: *Autophagy in Mammalian Systems, Volume 452 (Methods in Enzymology)*. Academic press 2009: 1-2.
38. Mizushima N, Yoshimori T, Levine B: *Methods in mammalian autophagy research*. *Cell* 2010; 140(3): 313-26.
39. Bross P, Gregersen N: *Methods in molecular biology (Protein misfolding and cellular stress in disease and aging-Springer Protocols)*. Humana press 2010: 198-204.
40. Rubinsztein DC, Cuervo AM, Ravikumar B, Sarkar S, Korolchuk V, Kaushik S, Klionsky DJ: *In search of an "autophagometer"*. *Autophagy* 2009; 5(5): 585-9.
41. Mizushima N, Yoshimori T: *How to interpret LC3 immunoblotting*. *Autophagy* 2007; 3(6): 542-5.
42. Otomo C, Metlagel Z, Takaesu G, Otomo T: *Structure of the human ATG12-ATG5 conjugate required for LC3 lipidation in autophagy*. *Nature structural & molecular biology* 2013; 20(1): 59-66.
43. Yang YP, Liang ZQ, Gu ZL, Qin ZH: *Molecular mechanism and regulation of autophagy*. *Acta pharmacologica sinica* 2005; 26(12): 1421-34.
44. Mizushima N, Yamamoto A, Hatano M, Kobayashi Y, Kabeya Y, Suzuki K, Tokuhiya T, Ohsumi Y, Yoshimori T: *Dissection of autophagosome formation using Apg5-deficient mouse embryonic stem cells*. *The journal of cell biology* 2001; 152(4): 657-68.
45. Romanov J, Walczak M, Ibricic I, Schüchner S, Ogris E, Kraft C, Martens S: *Mechanism and functions of membrane binding by the Atg5-Atg12/Atg16 complex during autophagosome formation*. *The EMBO journal* 2012; 31(22): 4304-17.
46. Noda NN, Fujioka Y, Hanada T, Ohsumi Y, Inagaki F: *Structure of the Atg12-Atg5 conjugate reveals a platform for stimulating Atg8-PE conjugation*. *EMBO reports* 2013; 14(2): 206-11.

47. Rubinstein AD, Eisenstein M, Ber Y, Bialik S, Kimchi A: *The autophagy protein Atg12 associates with antiapoptotic Bcl-2 family members to promote mitochondrial apoptosis*. *Molecular cell* 2011; 44(5): 698-709.
48. Shpilka T, Mizushima N, Elazar Z: *Ubiquitin-like proteins and autophagy at a glance*. *Journal of cell science* 2012; 125(Pt 10): 2343-8.
49. Mizushima N, Noda T, Yoshimori T, Tanaka Y, Ishii T, George MD, Klionsky DJ, Ohsumi M, Ohsumi Y: *A protein conjugation system essential for autophagy*. *Nature* 1998; 395(6700): 395-8.
50. Mizushima N, Kuma A, Kobayashi Y, Yamamoto A, Matsubae M, Takao T, Natsume T, Ohsumi Y, Yoshimori T: *Mouse Apg16L, a novel WD-repeat protein, targets to the autophagic isolation membrane with the Apg12-Apg5 conjugate*. *Journal of cell science* 2003; 116(Pt 9): 1679-88.
51. Karp G: *Cell and molecular biology*. Wiley 2008.
52. Lee HC, Wei YH: *Mitochondrial biogenesis and mitochondrial DNA maintenance of mammalian cells under oxidative stress*. *The international journal of biochemistry&cell biology* 2005; 37(4): 822-34.
53. Scarpulla RC, Vega RB, Kelly DP: *Transcriptional integration of mitochondrial biogenesis*. *Trends in endocrinology and metabolism* 2012; 23(9): 459-66.
54. Jornayvaz FR, Shulman GI: *Regulation of mitochondrial biogenesis*. *Essays in biochemistry* 2010; 47: 69-84.
55. Hock MB, Kralli A: *Transcriptional control of mitochondrial biogenesis and function*. *Annual review of physiology* 2009; 71: 177-203.
56. Mathew R, White E: *Autophagy, stress, and cancer metabolism: what doesn't kill you makes you stronger*. *Cold Spring Harbor symposia on quantitative biology* 2011; 76: 389-96.
57. Cirri P, Chiarugi P: *Tumors and their stroma: mitochondria at the crossroad*. *Cell cycle* 2013; 12(2): 204-5.

58. Luo C, Li Y, Wang H, Feng Z, Li Y, Long J, Liu J: *Mitochondrial accumulation under oxidative stress is due to defects in autophagy*. Journal of cellular biochemistry 2013; 114(1): 212-9.
59. Jawhar NM: *Tissue Microarray: A rapidly evolving diagnostic and research tool*. Annals of Saudi medicine 2009; 29(2): 123-7.
60. Gately K, Kerr K, O'Byrne K: *Design, construction, and analysis of cell line arrays and tissue microarrays for gene expression analysis*. Methods in molecular biology 2011; 784: 139-53.
61. <http://www.olympusconfocal.com/theory/confocalintro.html>, available in March 2014.
62. http://www.abcam.com/mitochondria-mtc02-antibody-ab3298.html#description_images_2, available in July 2013.
63. Eskelinen EL: *Roles of LAMP-1 and LAMP-2 in lysosome biogenesis and autophagy*. Molecular aspects of medicine 2006; 27(5-6): 495-502.
64. Deng Y, Wang CC, Choy KW, Du Q, Chen J, Wang Q, Li L, Chung TK, Tang T: *Therapeutic potentials of gene silencing by RNA interference: principles, challenges, and new strategies*. Gene 2014; 538(2): 217-27.
65. Aigner A: *Gene silencing through RNA interference (RNAi) in vivo: strategies based on the direct application of siRNAs*. Journal of biotechnology 2006; 124(1): 12-25.
66. Cufí S, Vazquez-Martin A, Oliveras-Ferraros C, Corominas-Faja B, Urruticoechea A, Martin-Castillo B, Menendez JA: *Autophagy-related gene 12 (ATG12) is a novel determinant of primary resistance to HER2-targeted therapies: utility of transcriptome analysis of the autophagy interactome to guide breast cancer treatment*. Oncotarget 2012; 3(12): 1600-14.
67. Edwards JL, Quattrini A, Lentz SI, Figueroa-Romero C, Cerri F, Backus C, Hong Y, Feldman EL: *Diabetes regulates mitochondrial biogenesis and fission in mouse neurons*. Diabetologia 2010; 53(1): 160-9.
68. Yuying Xie, Jun Li, Guibo Fan, Sihua Qi, Bing Li: *Reperfusion Promotes Mitochondrial Biogenesis following Focal Cerebral Ischemia in Rats*. PLoS one 2014; 9(3): e92443.